RESEARCH ARTICLE

Bifurcation and optimal control analysis of HIV/AIDS and COVID-19 co-infection model with numerical simulation

Belela Samuel Kotola [1,2] *, **Shewafera Wondimagegnhu Teklu** [2], **Yohannes Fissha Abebaw** [2]

1 Oda Bultum University, Chiro, Ethiopia, **2** Department of Mathematics, Natural Science, Debre Berhan University, Debre Berhan, Ethiopia

* belelasamuel@gmail.com, belelasmuel@dbu.edu.et

Abstract

HIV/AIDS and COVID-19 co-infection is a common global health and socio-economic problem. In this paper, a mathematical model for the transmission dynamics of HIV/AIDS and COVID-19 co-infection that incorporates protection and treatment for the infected (and infectious) groups is formulated and analyzed. Firstly, we proved the non-negativity and boundedness of the co-infection model solutions, analyzed the single infection models steady states, calculated the basic reproduction numbers using next generation matrix approach and then investigated the existence and local stabilities of equilibriums using Routh-Hurwiz stability criteria. Then using the Center Manifold criteria to investigate the proposed model exhibited the phenomenon of backward bifurcation whenever its effective reproduction number is less than unity. Secondly, we incorporate time dependent optimal control strategies, using Pontryagin's Maximum Principle to derive necessary conditions for the optimal control of the disease. Finally, we carried out numerical simulations for both the deterministic model and the model incorporating optimal controls and we found the results that the model solutions are converging to the model endemic equilibrium point whenever the model effective reproduction number is greater than unity, and also from numerical simulations of the optimal control problem applying the combinations of all the possible protection and treatment strategies together is the most effective strategy to drastically minimizing the transmission of the HIV/AIDS and COVID-19 co-infection in the community under consideration of the study.

1. Introduction

Infectious diseases are diagnostically proven illnesses caused by tiny microorganisms such as viruses, bacteria, fungi, and parasites and have been the leading causes of death throughout the world, for example; viruses cause both COVID-19 and HIV/AIDS infections [1–3].

Human immunodeficiency virus (HIV) is one of the most dangerous viruses that is spreading around the world. AIDS, or acquired immunodeficiency syndrome, is one of the most

devastating epidemics in history, caused by HIV, which has been a worldwide epidemic since 1981 [4–10]. It remains a significant world health issue that impacts almost seventy million people worldwide and has been a significant cause of morbidity and mortality [11,12]. HIV is transmissible through sexual contact, needle sharing, and direct contact with virus-infected blood or other body fluids, as well as from mother to child during giving birth [10,13–15].

In early December 2019, a coronavirus called COVID-19 was reported in Wuhan, China, with symptoms similar to pneumonia. According to reports, it is one of the most devastating infectious diseases caused by the novel coronavirus SARS-CoV-2, which has been a significant impact on the health, social, and economic integration of communities worldwide [16–29]. On March 11, 2020, the World Health Organization (WHO) confirmed it as a global pandemic, and on July 25, 2020, the world total number of COVID-19 infected individuals was 15,762,007, with 640,276 deaths [25,28,29]. It was suspected to be pneumonia or a common cold-like illness, with symptoms such as fatigue, alter in taste, fever, muscular pains, shortness of breath, ironical cough, and sore throat [25,27,30]. Despite massive efforts to reduce the virus's transmission and survivability, the death rate from COVID-19 remains high [15]. COVID-19 can be transmitted through sneezing or coughing droplets expelled from the human lungs, as well as when humans come into contact with contaminated dispatched materials [17,26,31]. Among the unfortunate aspects of the COVID-19 pandemic is that patients over the age of 60 are more likely to be infected than anyone below the age of 60 [31]. It is an extremely infectious contagious agent that has spread throughout most of the world's nations and has a significant impact on the global economy and public health [24,32]. COVID-19 infection may be more common in people with compromised immunity from other infections such as tuberculosis, HIV, pneumonia, and cholera [1,25,33–37]. WHO unanimously implemented vaccination, quarantine, wearing face masks, hand washing with alcohol, and significant discrepancies as possible prevention and control strategies [26,27,31]. Symptomless and pre-symptomatic transmission, a low incidence or lack of dominant systemic symptoms such as fever, airborne transmission that may require a high infectious dose and super-spread events are the essential aspects of COVID-19 spreading that make it challenging to handle [16].

A co-infection is the infection of a single individual with two or more different pathogens or different strains of the same pathogens, leading to co-existence of strains (pathogens) at population level [10]. Co-infection of two or more diseases in one individual is a regular occurrence in today's society [2,14]. Different researchers have investigated that COVID-19 infection could be high in people living with other infections like TB, HIV, and cholera who have compromised immunity [1,8,21,25,30,33–44].

Mathematical modelling approaches have been crucial to provide basic frameworks in order to understand the transmission dynamics of infectious diseases [37]. Many scholars throughout the world have been formulated and analyzed mathematical models to investigate the transmission dynamics of different infectious diseases using ordinary differential equations approach like [2,9,15,17,19,22,23,26–29,31,32,45–47] using stochastic approach like [48], and using fractional order derivative approach like [1,5,49,50]. In the structure of this study, we have reviewed research papers that have been done on the transmission dynamics of different infectious diseases especially co-infections of HIV/AIDS and other infectious diseases. Teklu and Rao [14] constructed and examined HIV/AIDS and pneumonia co-infection model with control measures such as pneumonia vaccination and treatments of pneumonia and HIV/AIDS infections. Hezam et al. [40], formulated a mathematical model for cholera and COVID-19 co-infection which describes the transmission dynamics of COVID-19 and cholera in Yemen. The model analysis examined four controlling measures such as social distancing, lockdown, the number of test kits to control the COVID-19 outbreak, and the number of

susceptible individuals who can get CWTs for water purification. Anwar et al. [15], constructed a mathematical model on COVID-19 with the isolation controlling measure on the COVID-19 infected individuals throughout the community. Ahmed et al. [1] formulated and analyzed HIV and COVID-19 co-infection model with ABC-fractional operator approach to investigate an epidemic prediction of a combined HIV-COVID-19 co-infection model. Numerical simulations were carried out to justify that the disease will stabilize at a later stage when enough protection strategies are taken. Teklu and Terefe [3] analyze COVID-19 and syphilis co-dynamics model to investigate the impacts of intervention measures on the disease transmission.

Similarly, various Scholars have formulated and analyzed mathematical models with optimal control strategies to investigate the effect of prevention and control measures on HIV/AIDS, COVID-19, HIV/AIDS and COVID-19 co-infection and other various infectious diseases transmission throughout nations in the world. For instance, Tchoumi et al. [37] proposed and investigated the co-dynamics of malaria and COVID-19 co-dynamics: with optimal control strategies. The numerical simulation results verifies the theoretical optimal control analysis and illustrates that using malaria and COVID-19 protection measures concurrently can help mitigate there transmission compared with applying single infections protection measures. Omame et al. [25] investigated a mathematical model for the dynamics of COVID-19 infection in order to assess the impacts of prior comorbidity on COVID-19 complications and COVID-19 reinfection with optimal control strategies. The authors recommended that the strategy that prevents COVID-19 infection by comorbid susceptible is the best cost-effective of all the other control strategies for the prevention of COVID-19. Ringa et al. [43] formulated and analyzed a mathematical model on HIV and COVID-19 co-infection with optimal control strategies. Their analysis suggested that COVID19 only prevention strategy is the most effective strategy and it averted about 10,500 new co-infection cases. Keno et al. [51] investigated an optimal control and cost effectiveness analysis of SIRS malaria disease model with temperature variability facto. Their result suggested that the combination of treatment of infected humans and insecticide spraying was proved to be the best efficient and least costly strategy to eradicate the disease. Keno et al. [52] investigated a mathematical model with optimal control strategies for malaria transmission with role of climate variability. Their result suggested that the combination of treated bed net and treatment is the most optimal and least-cost strategy to minimize the malaria. Goudiaby et al. [39] formulated and analyzed a COVID-19 and tuberculosis co-dynamics model with optimal control strategies. They suggested that COVID-19 prevention, treatment and control of co-infection yields a better outcome in terms of the number of COVID-19 cases prevented at a lower percentage of the total cost of this strategy. Asamoah et al. [53] constructed a mathematical model on COVID-19 to investigate optimal control strategies and comprehensive cost-effectiveness. Okosun et al. [54] formulated a mathematical model on HIV/AIDS to investigate the impact of optimal control on the treatment of HIV/AIDS and screening of unaware invectives. Their analysis recommended that the combination of all the control strategies is the most cost-effective strategy. Furthermore, notice that optimal control modeling and cost-effectiveness analysis model have been applied in recent infectious diseases models like [55,56].

As we observed from review of literatures done by various epidemiology and medical scholars, HIV/AIDS and COVID-19 co-infection is a public health concern especially in developing nations of the world. The main purpose of this paper is to investigate the impacts of COVID-19 protection with quarantine, COVID-19 treatment, HIV protection and HIV treatment prevention and controlling strategies on the transmission dynamics of HIV/AIDS and COVID-19 co-infection in the community with mathematical modelling approach. We have reviewed literatures [1,43] invested much effort in studying HIV/AIDS and COVID-19 co-infection, but

did not considered COVID-19 protection with quarantine, COVID-19 treatment, HIV/AIDS protection, and HIV/AIDS treatment as prevention and control strategies simultaneously in a single model formulation which motivates us to undertake this study and fill the gap.

2. Mathematical model construction

2.1. Basic frameworks of the model

In this paper, we partitioned the total human population at a given time t denoted by $N(t)$, into eleven mutually-exclusive classes depending on their infection status: susceptible class to both COVID-19 and HIV $S(t)$), COVID-19 protection by quarantine class ($C_q(t)$), HIV protected (such as by using condom, limit sexual partners, creating awareness etc.) class ($H_p(t)$), COVID-19 protection by vaccination class ($C_v(t)$), COVID-19 mono-infection class ($C_i(t)$), HIV unaware mono-infection class ($H_u(t)$), HIV aware mono-infection class ($H_a(t)$), HIV unaware and COVID-19 co-infection class ($M_u(t)$), HIV aware and COVID-19 co-infection class ($M_a(t)$), COVID-19 recovery class ($R(t)$), and HIV aware treatment class ($H_t(t)$) so that;

$$N(t) = S(t) + C_q(t) + H_p(t) + C_v(t) + C_i(t) + H_u(t) + H_a(t) + M_u(t) + M_a(t) + C_t(t) + R(t).$$

Since HIV is a chronic infectious disease the susceptible individuals acquires HIV infection at the standard incidence rate given by

$$\lambda_H(t) = \frac{\beta_1}{N}(H_u(t) + \rho_1 H_a(t) + \rho_2 M_u(t) + \rho_3 M_a(t)) \tag{1}$$

where $\rho_3 \geq \rho_2 \geq \rho_1 \geq 1$ are the modification parameters that increase infectivity and β_1 is the HIV transmission rate. Since COVID-19 is a very acute infection the susceptible individuals acquires COVID-19 infection at the mass action incidence rate as stated in [50,51,54].

$$\lambda_C(t) = \beta_2(C_i(t) + \omega_1 M_u(t) + \omega_2 M_a(t)) \tag{2}$$

where $\omega_2 > \omega_1 > 1$ are the modification parameters that increase infectivity and β_2 is the COVID-19 transmission rate.

Additional model assumptions

- k_1, k_2, k_3, and k_4 where $k_4 = 1 - k_1 - k_2 - k_3$ are portions of the number of recruited individuals those are entering to the susceptible class, the COVID-19 protected class, the HIV protected class and the COVID-19 vaccination class respectively.

- The susceptible class is increased by individuals from the COVID-19 vaccinated class in which those individuals who are vaccinated against COVID-19 but did not respond to vaccination with waning rate of ρ and from COVID-19 recovery with treatment class who develop their temporary immunity by the rate η.

- COVID-19 vaccine is may not be 100% efficient, so vaccinated individuals also have a chance of being infected with portion ε of the serotype not covered by the vaccine where $0 \leq \varepsilon < 1$.

- $0 < v \leq 1$ is the modification parameter such that COVID-19 infected individual is less susceptible to HIV infection than a susceptible individuals due to morbidity.

- There is screening and testing mechanisms for the previous and current status in each class.

- The human population distribution is homogeneous in each class.

- HIV treated individuals do not transmit infection to others due to awareness.

- Population of human being is variable.

Table 1. Biological meaning of model parameters.

Parameters	Biological definitions
μ	Human natural mortality rate
Δ	Recruitment of new born and immigrants
α_1	COVID-19 protection lose rate
α_2	HIV protection lose rate
ε	Proportion not covered by the COVID-19 vaccine
θ	Progression rate
ϕ_1, ϕ_2	Modification parameters
d_1	COVID-19 death rate
d_2	HIV/AIDS death rate for unaware
d_3	HIV/AIDS death rate for aware
κ	The rate at which COVID-19 infected are recovered by treatment
γ	HIV aware infection treatment rate
ρ	COVID-19 vaccination waning rate
υ	Modification parameter
β_1	HIV/AIDS transmission rate
β_2	COVID-19 transmission rate
k_1	Portion of recruitment entered to susceptible
k_2, k_3	Portion of recruitment entered to COVID-19 and HIV protections respectively
k_4	Portion of recruitment entered to COVID-19 vaccination class
δ	Co-infection progression rate
θ_1, θ_2	COVID-19 treatment rates
η	The rate at which recovered individuals loss temporary immunity
d_4, d_5	Co-infected death rates

https://doi.org/10.1371/journal.pone.0284759.t001

- There is no dual-infection transmission simultaneously.

- No vertical HIV transmission.

- No permanent immunity for COVID-19 infection.

In this section using parameters given in Table 1, model variables given in Table 2, and the model basic frame work, and assumptions given in (2.1), the schematic diagram for the transmission dynamics of HIV/AIDS and COVID-19 co-infection is given by Fig 1.

Table 2. Biological definitions of model variables.

| Variables	Biological Definitions
S	Susceptible class to both HIV and COVID-19 infections
C_q	Individuals who are protected by quarantine against COVID-19
H_p	Individuals who are protected against HIV infection
C_v	COVID-19 vaccinated class
C_i	COVID-19 infected class
H_u	Individuals mono-infected with HIV and unaware
H_a	Individuals mono-infected with HIV and aware
M_u	Co-infected individuals unaware of HIV infection
M_a	Co-infected individuals aware of HIV infection
R	COVID-19 recovered class
H_t	HIV/AIDS treated class

https://doi.org/10.1371/journal.pone.0284759.t002
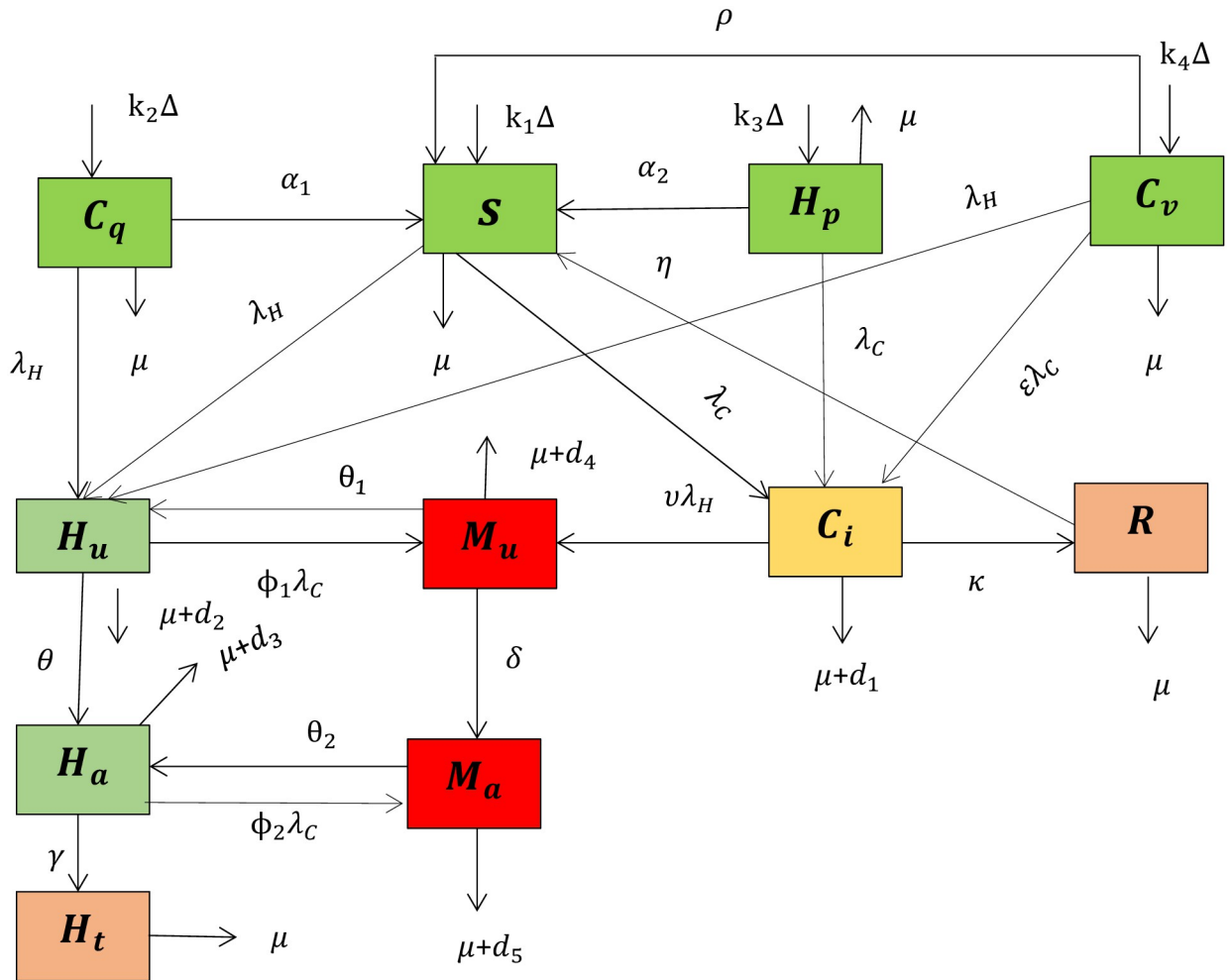
Fig 1. The schematic diagram of the HIV/AIDS and COVID-19 co-infection transmission dynamics.

https://doi.org/10.1371/journal.pone.0284759.g001

Now using Fig 1 the system of differential equations of the HIV/AIDS and COVID-19 co-infection is given by

$$
\begin{aligned}
\dot{S} &= k_1\Delta + \alpha_1 C_q + \alpha_2 H_p + \rho C_v + \eta R - (\lambda_H + \lambda_C + \mu)S, \\
\dot{C}_q &= k_2\Delta - (\lambda_H + \alpha_1 + \mu)C_q, \\
\dot{H}_p &= k_3\Delta - (\alpha_2 + \mu + \lambda_C)H_p, \\
\dot{C}_v &= k_4\Delta - (\rho + \mu + \lambda_H + \varepsilon\lambda_C)C_v, \\
\dot{C}_i &= \lambda_C S + \lambda_C C_q + \varepsilon\lambda_C C_v - (\mu + d_1 + \kappa + \upsilon\lambda_H)C_i, \\
\dot{H}_u &= \lambda_H S + \lambda_H C_q + \lambda_H C_v + \theta_1 M_u - (\theta + \mu + d_2 + \phi_1\lambda_C)H_u, \\
\dot{H}_a &= \theta H_u + \theta_2 M_a - (\gamma + d_3 + \mu + \phi_2\lambda_C)H_a, \\
\dot{M}_u &= \phi_1\lambda_C H_u + \upsilon\lambda_H C_i - (\mu + d_4 + \delta + \theta_1)M_u, \\
\dot{M}_a &= \delta M_u + \phi_2\lambda_C H_a - (\mu + d_5 + \theta_2)M_a, \\
\dot{R} &= \kappa C_i - (\mu + \eta)R, \\
\dot{H}_t &= \gamma H_a - \mu H_t,
\end{aligned}
\tag{3}
$$

with the corresponding initial conditions

$$S(0) > 0, C_q(0) \geq 0, \ H_p(0) \geq 0, \ C_v(0) \geq 0, C_i(0) \geq 0, H_u(0) \geq 0, H_a(0) \geq 0, M_u(0)$$
$$\geq 0, M_a(0) \geq 0, \ R > 0, \ \text{and } H_t > 0. (4)$$

The sum of all the differential equations in (3) is

$$\dot{N} = \Delta - \mu N - (d_1 C_i + d_2 H_u + d_3 H_a + d_4 M_u + d_5 M_a). \tag{5}$$

2.2. The basic qualitative properties of the model (3)

The COVID-19 and HIV/AIDS co-infection model given in Eq (3) is both biologically and mathematically meaningful if and only if all the model solutions (state variables) are non-negative and bounded in the invariant region

$$\Omega = \left\{ \left(S, \ C_q, H_p, C_v, \ C_i, \ H_u, \ H_a, \ M_u, M_a, R, \ H_t\right) \in \mathbb{R}_+^{11}, N \leq \frac{\boldsymbol{\Lambda}}{\boldsymbol{\mu}} \right\} \tag{6}$$

Theorem 1 (**Positivity of the model solutions**)

Let us given the initial data in Eq (4) then the solutions $S(t)$, $H_p(t)$, $C_v(t)$, $C_i(t)$, $M_u(t)$, $H_u(t)$, $H_a(t)$, $M_a(t)$, $R(t)$, $C_q(t)$, and $H_t(t)$ of the COVID-19 and HIV/AIDS co-infection model (3) are nonnegative for all time $t > 0$.

Proof: Let us consider $S(0) > 0, C_q(0) > 0, H_p(0) > 0, C_v(0) > 0, C_i(0) > 0, H_u(0) > 0, H_a(0) > 0, M_u(0) > 0, M_a(0) > 0, R(0) > 0,$ and $Ht(0) > 0$ then for all t > 0.

We have to show that $S(t) > 0, C_q(t) > 0, H_p(t) > 0, C_v(t) > 0, C_i(t) > 0, H_u(t) > 0, H_a(t) > 0, M_u(t) > 0, M_a(t) > 0, R(0) > 0,$ and $H_t(t) > 0$.

Define: $\tau = \sup\{S(t) > 0, C_q(t) > 0, H_p(t) > 0, C_v(t) > 0, C_i(t) > 0, H_u(t) > 0, H_a(t) > 0, M_u(t) > 0, M_a(t) > 0, R(0) > 0,$ and $H_t(t) > 0\}$. Now since the entire co-infection model state variables are positive and all the state variables are continuous, we can justify that $\tau > 0$. If $\tau = +\infty$, then non-negativity holds. But, if $0 < \tau < +\infty$ we will have $S(\tau) = 0$ or $C_q(\tau) = 0$ or $H_p(\tau) = 0$ or $C_v(\tau) = 0$ or $C_i(\tau) = 0$ or $H_u(\tau) =$ or $H_a(\tau) = 0$ or $M_u(\tau) = 0$ or $M_a(\tau) = 0$ or $R(\tau) = 0$ or $H_t(\tau) = 0$.

Here from the first equation of the COVID-19 and HIV/AIDS co-infection model (3) we have got

$$\dot{S} + (\lambda_H + \lambda_C + \mu)S = k_1\Delta + \alpha_1 C_q + \alpha_2 H_p + \rho C_v + \eta R.$$

and integrate using method of integrating factor we have determined the constant value

$$S(\tau) = M_1 S(0) + M_1 \int_0^\tau exp^{\int (\mu + \lambda_H(t) + \lambda_C(t))dt} \left(\alpha_1 C_q + \alpha_2 H_p + \rho C_v + \eta R\right) dt > 0$$

where

$$M_1 = exp^{-\left(\mu\tau + \int_0^\tau (\lambda_H(w) + \lambda_C(w))\right)} > 0, \ S(0) > 0,$$

and from the meaning of τ, the solutions $C_q(t) > 0, H_p(t) > 0, C_v(t) > 0, R(t) > 0$. Moreover, the exponential function is always positive, then the solution $S(\tau) > 0$ hence $S(\tau) \neq 0$. Thus following the same procedure for $\tau = +\infty$, all the solutions of the COVID-19 and HIV/AIDS co-infection system (3) are non-negative.

Theorem 2 (The invariant region): All the feasible positive solutions of the co-infection model (3) are bounded in the region (6).

Proof: Let $\left(S, C_q, H_p, C_v, C_i, H_u, H_a, M_u, M_a, R, H_t\right) \in \mathbb{R}_+^{11}$ is an arbitrary non-negative solution of the system (3) with initial conditions given in Eq (4). Now adding all the differential equations given in Eq (3) we have got the derivative of the total population N which is given in Eq (5) as

$$\dot{N} = \Delta - \mu N - (d_1 C_i + d_2 H_u + d_3 H_a + d_4 M_u + d_5 M_a).$$

Then by ignoring the infections we have determined that $\dot{N} \le \Delta - \mu N$ and using separation of variables whenever $t \to \infty$, we have obtained that $0 \le N \le \frac{\Delta}{\mu}$. Hence, all the positive feasible solutions of the co-infection model (3) entering in to the region given in Eq (6).

Note: Since the model (3) solutions are both positive and bounded in the region (6) the HIV/AIDS and COVID-19 co-infection model (3) is both mathematically and biologically meaning full [45,47,57], then we can consider the two mono-infection models, namely; HIV mono-infection and COVID-19 mono-infection models. This is fundamental for the analysis of the COVID-19 and HIV/AIDS co-infection model.

3. Analytical result of the models

Before analyzing the HIV/AIDS and COVID-19 co-infection model given in Eq (3), it is very crucial to gain some basic backgrounds about the COVID-19 and HIV/AIDS mono-infection models.

3.1. Mathematical analysis of HIV/AIDS mono-infection model

In this subsection we assume there is no COVID-19 infection in the community i.e. $C_q =$, $C_q = C_i = M_u = M_a = R = 0$ in (3) then the HIV/AIDS sub-model is given by

$$\left. \begin{aligned} \dot{S} &= k_1 \Delta + \alpha_2 H_p - (\lambda_H + \mu) S \\ \dot{H}_p &= k_3 \Delta - (\alpha_2 + \mu) H_p \\ \dot{H}_u &= \lambda_H S - (\theta + \mu + d_2) H_u \\ \dot{H}_a &= \theta H_u - (\gamma + d_3 + \mu) H_a \\ \dot{H}_t &= \gamma H_u - \mu H_t, \end{aligned} \right\} \tag{7}$$

where the total population $N_1(t) = S(t) + H_p(t) + H_u(t) + H_a(t) + H_t(t)$, and the HIV sub-model force of infection given by $\lambda_H = \frac{\beta_1}{N_1}(H_u + \rho_1 H_a)$ and initial conditions $S(0) > 0, H_p(0) \ge 0$, $H_a(0) \ge 0, H_u(0) \ge 0$ and $H_t(0) \ge 0$. In a similar manner of the full co-infection model (3) in the region $\Omega_1 = \left\{ \left(S, H_p, H_u, H_a, H_t\right) \in \mathbb{R}_+^5, N_1 \le \frac{\Delta}{\mu} \right\}$, it is sufficient to consider the dynamics of the sub-model (7) in Ω_1 as biologically and mathematically well-posed.

3.2. Disease-free equilibrium point of HIV mono-infection model (7) local stability

The disease-free equilibrium point of the HIV mono-infection system in (7) is obtained by making its right-hand side is equal to zero and setting the infected classes and treatment class to zero as $H_u = H_a = H_t = 0$ which yields, $S^O = \frac{k_1 \Delta(\alpha_2 + \mu) + \alpha_2 k_3 \Delta}{\mu(\alpha_2 + \mu)}$, $H_p^0 = \frac{k_3 \Delta}{\alpha_2 + \mu}$. Hence the disease-free equilibrium point is given by $E_{HM}^0 = \left(S^0, H_p^0, H_u^0, H_a^0, H_t^0\right) = \left(\frac{k_1 \Delta(\alpha_2 + \mu) + \alpha_2 k_3 \Delta}{\mu(\alpha_2 + \mu)}, \frac{k_3 \Delta}{\alpha_2 + \mu}, 0, 0, 0\right)$.

The local stability of the HIV mono-infection model (7) disease-free equilibrium point is examined by its effective reproduction number denoted by $\mathcal{R}_{HM}$, which is calculated by using the next generation operator method determined by Van den Driesch and Warmouth stated in [2]. Applying the method stated in [29], the transmission matrix F and the transition matrix V i.e., for the new infection and the remaining transfer respectively, are given by

$$F = \begin{bmatrix} \dfrac{\beta_1 \theta S^0}{S^O + H_p^0} & \dfrac{\beta_1 \rho_1 \theta S^0}{S^O + H_p^0} & 0 \\ 0 & 0 & 0 \\ 0 & 0 & 0 \end{bmatrix} \text{ and } V = \begin{bmatrix} \theta + \mu + d_2 & 0 & 0 \\ -\theta & \gamma + d_3 + \mu & 0 \\ 0 & -\gamma & \mu \end{bmatrix}.$$

After some computations we have determined that

$$V^{-1} = \begin{bmatrix} \dfrac{1}{(\theta + \mu + d_2)} & 0 & 0 \\ \dfrac{\theta}{(\theta + \mu + d_2)(\gamma + \mu + d_3)} & \dfrac{1}{(\gamma + \mu + d_3)} & 0 \\ \dfrac{\gamma \theta}{\mu(\theta + \mu + d_2)(\gamma + \mu + d_3)} & \dfrac{\gamma}{\mu(\gamma + \mu + d_3)} & \dfrac{1}{\mu} \end{bmatrix},$$

and

$$FV^{-1} = \begin{bmatrix} \dfrac{\beta_1 S^0}{(S^0 + H_p^0)((\theta + \mu + d_2))} + \dfrac{\beta_1 \rho_1 \theta S^0}{\left(S^0 + H_p^0\right)(\theta + \mu + d_2)(\gamma + \mu + d_3)} & \dfrac{\beta_1 \rho_1 \theta S^0}{\left(S^0 + H_p^0\right)(\gamma + \mu + d_3)} & 0 \\ 0 & 0 & 0 \\ 0 & 0 & 0 \end{bmatrix}.$$

Then, the effective reproduction number of the HIV mono-infection model (7) is defined as the largest eigenvalue in magnitude of the next generation matrix, FV^{-1} given by

$$\mathcal{R}_{HM} = \frac{\beta_1(1 - k_3)(\alpha_2 + \mu) + \beta_1 \alpha_2 k_3}{(\alpha_2 + \mu)(\theta + \mu + d_2)} + \frac{\beta_1 \rho_1 \theta(1 - k_3)(\alpha_2 + \mu) + \beta_1 \rho_1 \theta \alpha_2 k_3}{(\theta + \mu + d_2)(\gamma + \mu + d_3)}.$$

The value $\mathcal{R}_{HM}$ is defined as the total average number of secondary HIV unaware and HIV aware infection cases acquired from a typical HIV unaware or HIV aware individual during his/her effective infectious period in a susceptible population. The threshold result $\mathcal{R}_{HM}$ is the effective reproduction number for HIV mono-infection.

Theorem 3: The disease-free equilibrium point of the HIV mono-infection model given in Eq (7) is locally asymptotically stable (LAS) if $\mathcal{R}_{HM} < 1$, and it is unstable if $\mathcal{R}_{HM} > 1$.

Proof: The local stability of the disease-free equilibrium point of HIV mono-infection model (7) is evaluated by applying the Routh-Hurwitz stability criteria stated in [52].

The Jacobian matrix of the HIV mono-infection model given in Eq (7) at the disease-free equilibrium point E_{HM}^0 is given by

$$J(E_{HM}^0) = \begin{bmatrix} -\mu & \alpha_2 & -\dfrac{\beta_1 S^0}{S^0 + H_p^0} & -\dfrac{\beta_1 S^0 \rho_1}{S^0 + H_p^0} & 0 \\ 0 & -(\alpha_2 + \mu) & 0 & 0 & 0 \\ 0 & 0 & \dfrac{\beta_1 S^0}{S^0 + H_p^0} - (\theta + \mu + d_2) & \dfrac{\beta_1 S^0 \rho_1}{S^0 + H_p^0} & 0 \\ 0 & 0 & \theta & -(\gamma + d_3 + \mu) & 0 \\ 0 & 0 & 0 & \gamma & -\mu \end{bmatrix}.$$

Then the corresponding characteristic equation of the Jacobian matrix $J(E_{HM}^0)$ is given by

$$\begin{vmatrix} -\mu - \lambda & \alpha_2 & -\dfrac{\beta_1 S^0}{S^0 + H_p^0} & -\dfrac{\beta_1 S^0 \rho_1}{S^0 + H_p^0} & 0 \\ 0 & -(\alpha_2 + \mu) - \lambda & 0 & 0 & 0 \\ 0 & 0 & \dfrac{\beta_1 S^0}{S^0 + H_p^0} - (\theta + \mu + d_2) - \lambda & -\dfrac{\beta_1 S^0}{S^0 + H_p^0} & 0 \\ 0 & 0 & \theta & -(\gamma + d_3 + \mu) - \lambda & 0 \\ 0 & 0 & 0 & \gamma & -\mu - \lambda \end{vmatrix} = 0,$$

$$\Rightarrow (-\mu - \lambda)(-(\alpha_2 + \mu) - \lambda)(-\mu - \lambda)\left[\left(-\dfrac{\beta_1 S^0}{S^0 + H_p^0} - (\theta + \mu + d_2) - \lambda\right)(-(\gamma + d_3 + \mu) - \lambda) - \dfrac{\theta \beta_1 S^0 \rho_1}{S^0 + H_p^0}\right]$$

$$= 0.$$

Finally we have determined

$$(-\mu - \lambda)(-(\alpha_2 + \mu) - \lambda)(-\mu - \lambda)(\lambda^2 + a\lambda + b) = 0,$$

where $a = (\gamma + d_3 + \mu) + (\theta + \mu + d_2) - \dfrac{\beta_1 S^0}{S^0 + H_p^0}$, and $b =$

$-\left(\dfrac{\beta_1 S^0}{S^0 + H_p^0} - (\theta + \mu + d_2)\right)(\gamma + d_3 + \mu) - \dfrac{\theta \beta_1 S^0 \rho_1}{S^0 + H_p^0} = (\theta + \mu + d_2)(\gamma + d_3 + \mu) -$

$(\gamma + d_3 + \mu)\dfrac{\beta_1 S^0}{S^0 + H_p^0} - \dfrac{\theta \beta_1 S^0 \rho_1}{S^0 + H_p^0} = (\theta + \mu + d_2)(\gamma + d_3 + \mu)\left(1 - \dfrac{\beta_1 \rho_1 \theta (1-k_3)(\alpha_2 + \mu) + \beta_1 \rho_1 \theta \alpha_2 k_3}{(\theta + \mu + d_2)(\gamma + \mu + d_3)}\right) =$

$(\theta + \mu + d_2)(\gamma + d_3 + \mu)(1 - \mathcal{R}_{HM})$.

Then we have got $\lambda_1 = -\mu < 0$ or $\lambda_2 = -(\alpha_2 + \mu) < 0$ or $\lambda_3 = -\mu < 0$ or

$$\lambda^2 + a\lambda + b = 0 \tag{8}$$

On Eq (8) we applied Routh-Hurwitz stability criteria stated in [47] and we have determined that both eigenvalues are negative if $\mathcal{R}_{HM} < 1$. Furthermore, we can conclude that the disease-free equilibrium point of the model (7) is locally asymptotically stable whenever $\mathcal{R}_{HM} < 1$ since all the eigenvalues are negative when $\mathcal{R}_{HM} < 1$. The biological meaning of Theorem 3 can be stated as HIV infection can be eradicated from the population (whenever $\mathcal{R}_{HM} < 1$) if the initial size of the sub-populations of the HIV mono-infection model given in Eq (7) is in the basin of attraction of the disease-free equilibrium point E_{HM}^0.

3.3. Existence of HIV mono-infection endemic equilibrium point(s)

Let $E_{HM}^* = \left(S^*, H_p^*, H_u^*, H_a^*, H_t^*\right)$ be an arbitrary endemic equilibrium point of the HIV mono-infection model (7) which can be determined by making the right hand side of Eq (7) as zero. The after a number of steps of computations we have got

$$S^* = \frac{k_1 \Delta m_1 + \alpha_2 k_3 \Delta}{m_1\left(\lambda_H^* + \mu\right)}, \quad H_p^* = \frac{k_3 \Delta}{m_1}, \quad H_u^* = \frac{k_1 \Delta m_1 \lambda_H^* + \alpha_2 k_3 \Delta \lambda_H^*}{m_1 m_2\left(\lambda_H^* + \mu\right)},$$

$$H_a^* = \frac{k_1 \Delta \theta m_1 \lambda_H^* + \alpha_2 k_3 \Delta \theta \lambda_H^*}{m_1 m_2 m_3\left(\lambda_H^* + \mu\right)}, \quad H_t^* = \frac{k_1 \Delta \theta \gamma m_1 \lambda_H^* + \alpha_2 k_3 \Delta \theta \gamma \lambda_H^*}{\mu m_1 m_2 m_3\left(\lambda_H^* + \mu\right)},$$
(9)

where $m_1 = (\alpha_2 + \mu)$, $m_2 = (\theta + \mu + d_2)$, and $m_3 = (\gamma + d_3 + \mu)$.

Now substitute H_u^* and H_a^* given in Eq (9) in to the HIV/AIDS force of infection

$$\lambda_H^* = \frac{\beta_1 H_u^* + \rho_1 H_a^*}{S^* + H_p^* + H_u^* + H_a^* + H_t^*}.$$

Then we have the result

$$(m_5 + m_6 \lambda_H^* - m_4)\lambda_H^* = 0.$$
(10)

where $m_4 = \beta_1 k_1 \Delta m_1 m_3 m_3 \mu + \beta_1 \alpha_2 k_3 \Delta m_3 m_3 \mu + \beta_1 \rho_1 k_1 \Delta \theta m_1 m_3 \mu + \beta_1 \rho_1 \alpha_2 k_3 \Delta \theta m_3 \mu$, $m_5 = k_1 \Delta m_1 m_2 m_3 \mu + \alpha_2 k_3 \Delta m_2 m_3 \mu + k_3 \Delta m_2 m_3 \mu\mu$, $m_6 = k_3 \Delta m_2 m_3 \mu + k_1 \Delta m_1 m_3 \mu + \alpha_2 k_3 \Delta m_3 \mu + k_1 \Delta \theta m_1 \mu + \alpha_2 k_3 \Delta \theta \mu + k_1 \Delta \theta \gamma m_1 + \alpha_2 k_3 \Delta \theta \gamma$.

Then the non-zero solution of (10) is $\lambda_H^* = \frac{m_4 - m_5}{m_6}$. Therefore, the required non-zero solution (force of infection is obtained as $\lambda_H^* = \frac{[k_1 \Delta m_1 m_2 m_3 \mu + k_3 \Delta m_2 m_3 \mu(\alpha_2 + \mu)](\mathcal{R}_{HM} - 1)}{k_3 \Delta m_2 m_3 \mu + k_1 \Delta m_1 m_3 \mu + \alpha_2 k_3 \Delta m_3 \mu + k_1 \Delta \theta m_1 \mu + \alpha_2 k_3 \Delta \theta \mu + k_1 \Delta \theta \gamma m_1 + \alpha_2 k_3 \Delta \theta \gamma}$. Then we have got $\lambda_H^* > 0$ whenever $\mathcal{R}_{HM} > 1$. Thus, the HIV/AIDS mono-infection model (7) has a unique positive endemic equilibrium point if and only if $\mathcal{R}_{HM} > 1$.

Theorem 4: The HIV/AIDS mono-infection model given in (7) has a unique endemic equilibrium point if and only if $\mathcal{R}_{HM} > 1$.

3.4. COVID-19 sub-model analysis

The corresponding COVID-19 sub-model of the system (3) is determined by making $H_p = H_a = H_u = M_u = M_a = H_t = 0$, and it is given by

$$\left.\begin{aligned}
\dot{S} &= k_1 \Delta + \alpha_1 C_q + \rho C_v + \eta R - (\lambda_C + \mu)S, \\
\dot{C}_q &= k_2 \Delta - (\alpha_1 + \mu)C_q, \\
\dot{C}_v &= k_4 \Delta - (\rho + \mu + \varepsilon\lambda_C)C_v, \\
\dot{C}_i &= \lambda_C S + \varepsilon\lambda_C C_v - (\mu + d_1 + \kappa)C_i, \\
\dot{R} &= \kappa C_i - (\mu + \eta)R,
\end{aligned}\right\}$$
(11)

with COVID-19 infection initial conditions $S(0) > 0, C_q(0) \geq 0, C_v(0) \geq 0, C_i(0) \geq 0, R(0) \geq 0$, total population $N_2(t) = S(t) + C_q(t) + C_v(t) + C_i(t) + R(t)$, and COVID-19 force of infection given by $\lambda_C = \beta_2 C_i(t)$. Here like the full model (3) and the HIV/AIDS sub-model (7) in the region $\Omega_2 = \left\{\left(S, C_q, C_v, C_i, R\right) \in \mathbb{R}^5_+, N_2 \leq \frac{\Delta}{\mu}\right\}$, it is sufficient to consider the dynamics of model (11) in Ω_2 be both biologically and mathematically meaningful.

3.4.1. Local stability of COVID-19 mono-infection model (11) Disease-free equilibrium. Disease-free equilibrium point of the COVID-19 mono-infection model (11) is

obtained by making its right-hand side as zero and setting the infected class and recovered with treatment class to zero as $C_i = R = 0$ and after some simple steps of calculations we have determined that $S^0 = \frac{k_1\Delta(\alpha_1+\mu)(\rho+\mu)+\alpha_1 k_2\Delta(\rho+\mu)+k_4\Delta\rho(\alpha_1+\mu)}{\mu(\alpha_1+\mu)(\rho+\mu)}$, $C_q^0 = \frac{k_2\Delta}{\alpha_1+\mu}$, and $C_i^0 = \frac{k_4\Delta}{\rho+\mu}$. Hence the COVID-19 mono-infection model (11) disease-free equilibrium point is given by

$$E_{PM}^0 = (S^0, C_q^0, C_v^0, C_i^0, R^0)$$
$$= \left(\frac{k_1\Delta(\alpha_1+\mu)(\rho+\mu)+\alpha_1 k_2\Delta(\rho+\mu)+k_4\Delta\rho(\alpha_1+\mu)}{\mu(\alpha_1+\mu)(\rho+\mu)}, \frac{k_2\Delta}{\alpha_1+\mu}, \frac{k_4\Delta}{>\rho+\mu}, 0, 0\right).$$

Here we are applying the Van Den Driesch and Warmouth next-generation matrix approach stated in [2] to determine the COVID-19 mono-infection model (11) effective reproduction number $\mathcal{R}_C$. After long computations, we have determined the transmission matrix given by

$$F = \begin{bmatrix} \beta_2 S^0 + \varepsilon\beta_2 C_i^0 & 0 \\ 0 & 0 \end{bmatrix},$$

and the transition matrix given by

$$V = \begin{bmatrix} \mu + d_1 + \kappa & 0 \\ -\kappa & \mu + \eta \end{bmatrix}.$$

Then using Mathematica we have determined as

$$V^{-1} = \begin{bmatrix} \dfrac{1}{\mu + d_1 + \kappa} & 0 \\ \dfrac{\kappa}{(\mu + d_1 + \kappa)(\mu + \eta)} & \dfrac{1}{\mu + \eta} \end{bmatrix} \text{ and } FV^{-1} = \begin{bmatrix} \dfrac{\beta_2 S^0 + \varepsilon\beta_2 C_i^0}{\mu + d_1 + \kappa} & 0 \\ 0 & 0 \end{bmatrix}.$$

The characteristic equation of the matrix FV^{-1} is $\begin{vmatrix} \dfrac{\beta_2 S^0 + \varepsilon\beta_2 C_i^0}{\mu + d_1 + \kappa} - \lambda & 0 \\ 0 & 0 - \lambda \end{vmatrix} = 0.$

Then the spectral radius (effective reproduction number $\mathcal{R}_C$) of FV^{-1} of the COVID-19 mono-infection model (11) is $\mathcal{R}_C = \frac{\beta_2 S^0 + \varepsilon\beta_2 C_i^0}{\mu + d_1 + \kappa} = \frac{\beta_2 k_1\Delta(\alpha_1+\mu)(\rho+\mu)+\beta_2\alpha_1 k_2\Delta(\rho+\mu)+\beta_2 k_4\Delta\rho(\alpha_1+\mu)+\beta_2\varepsilon k_4\Delta\mu(\alpha_1+\mu)}{\mu(\alpha_1+\mu)(\rho+\mu)(\mu+d_1+\kappa)}$.

Theorem 5: The Disease-free equilibrium point E_{CM}^0 of the COVID-19 mono-infection model (11) is locally asymptotically stable if $\mathcal{R}_C < 1$ otherwise unstable.

Proof: The local stability of the disease-free equilibrium of the system (11) at point $E_{CM}^0 = \left(\frac{k_1\Delta(\alpha_1+\mu)(\rho+\mu)+\alpha_1 k_2\Delta(\rho+\mu)+k_4\Delta\rho(\alpha_1+\mu)}{\mu(\alpha_1+\mu)(\rho+\mu)}, \frac{k_2\Delta}{\alpha_1+\mu}, \frac{k_4\Delta}{\rho+\mu}, 0, 0\right)$ can be studied from its Jacobian matrix and Routh-Hurwitz stability criteria. The Jacobian matrix of the dynamical system at the disease-

free equilibrium point is given by

$$J\left(E_{CM}^0\right) = \begin{bmatrix} -\mu & \alpha_1 & \rho & -\beta_2 S^0 & \eta \\ 0 & -(\alpha_1 + \mu) & 0 & 0 & 0 \\ 0 & 0 & -(\rho + \mu) & -\beta_2 \varepsilon C_i^0 & 0 \\ 0 & 0 & 0 & \beta_2 A_1^0 + \beta_2 \varepsilon C_i^0 - (\mu + d_1 + \kappa) & 0 \\ 0 & 0 & 0 & \kappa & -(\mu + \eta) \end{bmatrix}.$$

Then the characteristic equation of the above Jacobian matrix is given by

$$\begin{vmatrix} -\mu & \alpha_1 & \rho & -\beta_2 S^0 & \eta \\ 0 & -(\alpha_1 + \mu) & 0 & 0 & 0 \\ 0 & 0 & -(\rho + \mu) & -\beta_2 \varepsilon C_i^0 & 0 \\ 0 & 0 & 0 & M & 0 \\ 0 & 0 & 0 & \kappa & -(\mu + \eta) \end{vmatrix} = 0,$$

where $M = \beta_2 S^0 + \beta_2 \varepsilon C_i^0 - (\mu + d_1 + \kappa)$ and after some steps of computations we have got $\lambda_1 = -\mu < 0$ or $\lambda_2 = -(\alpha_1 + \mu) < 0$ or $\lambda_3 = -(\rho + \mu) < 0$ or $\lambda_4 = \beta_2 S^0 + \beta_2 \varepsilon C_i^0 - (\mu + d_1 + \kappa) = (\mu + d_1 + \kappa)\left[\frac{\beta_2 S^0 + \beta_2 \varepsilon C_i^0}{\mu + d_1 + \kappa} - 1\right] = \mu + d_1 + \kappa)[\mathcal{R}_C - 1] < 0$ if $\mathcal{R}_C < 1$ or $\lambda_5 = -(\mu + \eta) < 0$.

Therefore, since all the eigenvalues of the characteristics polynomials of the system (11) are negative if $\mathcal{R}_C < 1$ the disease-free equilibrium point of the COVID-19 mono-infection model (11) is locally asymptotically stable.

3.4.2. Existence of endemic equilibrium point (s) of the COVID-19 mono-infection model. Before checking the global stability of the disease-free equilibrium point of the COVID-19 mono-infection model (11), we shall find the possible number of endemic equilibrium point(s) of the model (11). Let $E_C^* = (S^*, C_q^*, C_v^*, C_i^*, R^*)$ be the endemic equilibrium point of COVID-19 mono-infection and $\lambda_C^* = \beta_2 C_i^*$ be the COVID-19 mono-infection mass action incidence rate ("force of infection") at the equilibrium point. To find equilibrium point (s) for which COVID-19 mono-infection is endemic in the population, the equations are solved in terms of $\lambda_C^* = \beta_2 C_i^*$ at an endemic equilibrium point. Now setting the right-hand sides of the equations of the model to zero (at steady state) gives

$$S^* = \frac{b_5\left(b_2 + \varepsilon\lambda_C^*\right)^2 + b_6\left(b_2 + \varepsilon\lambda_C^*\right)^2 + b_7\left(b_2 + \varepsilon\lambda_C^*\right) + b_8\lambda_C^*}{b_1 b_3 b_4\left(b_2 + \varepsilon\lambda_C^*\right)^2\left(\lambda_C^* + \mu\right) - b_1 \eta\kappa\left(b_2 + \varepsilon\lambda_C^*\right)^2\lambda_C^*}, \quad C_q^* = \frac{k_2\Delta}{b_1}, \quad C_v^* = \frac{k_4\Delta}{\left(b_2 + \varepsilon\lambda_C^*\right)},$$

$$C_i^* = \frac{b_5\left(b_2 + \varepsilon\lambda_C^*\right)^2\lambda_C^* + b_6\left(b_2 + \varepsilon\lambda_C^*\right)^2\lambda_C^* + \left(b_2 b_7\lambda_C^* + b_7\varepsilon\lambda_C^{*2}\right)}{b_{12}\left(b_2 + \varepsilon\lambda_C^*\right)^2\left(\lambda_C^* + \mu\right) - b_{13}\left(b_2 + \varepsilon\lambda_C^*\right)^2\lambda_C^*} + \frac{b_8\lambda_C^{*2} + \left(b_2 b_9 + b_9\varepsilon\lambda_C^*\right)\left(\lambda_C^{*2} + \mu\lambda_C^*\right) - b_{10}\lambda_C^{*2} - b_{11}\lambda_C^{*3}}{b_{12}\left(b_2 + \varepsilon\lambda_C^*\right)^2\left(\lambda_C^* + \mu\right) - b_{13}\left(b_2 + \varepsilon\lambda_C^*\right)^2\lambda_C^*},$$

and

$$R^* = \frac{\kappa B_5^*}{b_4},$$

where $b_1 = \alpha_1 + \mu$, $b_2 = \rho + \mu$, $b_3 = \mu + d_1 + \kappa$, $b_4 = \mu + \eta$, $b_5 = k_1\Delta b_1 b_3 b_4$, $b_6 = \alpha_1 k_2\Delta b_3 b_4$, $b_7 = $

$\rho k_4 \Delta b_1 b_3 b_4$, $b_8 = k_4 \Delta b_1 \eta \kappa \varepsilon$, $b_9 = b_1 b_3 b_4 k_4 \Delta \varepsilon$, $b_{10} = b_2 b_1 \eta \kappa k_4 \Delta \varepsilon$, $b_{11} = b_1 k_4 \Delta \varepsilon \eta \kappa \varepsilon$, $b_{12} = b_1 b_3 b_3 b_4$, $b_{13} = b_1 b_3 \eta \kappa$.

Then we have substituted $C_i^* = \frac{b_5 \left(b_2 + \varepsilon \lambda_C^*\right)^2 \lambda_C^* + b_6 \left(b_2 + \varepsilon \lambda_C^*\right)^2 \lambda_C^* + \left(b_2 b_7 \lambda_C^* + b_7 \varepsilon \lambda_C^{*2}\right)}{b_{12} \left(b_2 + \varepsilon \lambda_C^*\right)^2 \left(\lambda_C^* + \mu\right) - b_{13} \left(b_2 + \varepsilon \lambda_C^*\right)^2 \lambda_C^*} +$

$\frac{b_8 \lambda_C^{*2} + \left(b_2 b_9 + b_9 \varepsilon \lambda_C^*\right)\left(\lambda_C^{*2} + \mu \lambda_C^*\right) - b_{10} \lambda_C^{*2} - b_{11} \lambda_C^{*3}}{b_{12} \left(b_2 + \varepsilon \lambda_C^*\right)^2 \left(\lambda_C^* + \mu\right) - b_{13} \left(b_2 + \varepsilon \lambda_C^*\right)^2 \lambda_C^*}$ in the COVID-19 force of infection given by $\lambda_C^* = \beta_2 R^*$ we have got the non-zero solution of λ_C^* is obtained from the cubic equation

$$c_3 \lambda_C^{*3} + c_2 \lambda_C^{*2} + c_1 \lambda_C^* + a_0 = 0, \tag{12}$$

where

$$
\begin{aligned}
&c_3 = b_{12} \varepsilon^2 - b_{13} \varepsilon^2 > 0 \\
&c_2 = 2 b_2 b_{12} \varepsilon + b_{12} \mu \varepsilon^2 - 2 b_2 b_{13} \varepsilon - b_5 \varepsilon^2 - b_6 \varepsilon^2 - b_9 \varepsilon + b_{11}, \\
&c_1 = b_2^2 b_{12} + b_{10} + 2 b_2 b_{12} \varepsilon \mu - b_2^2 b_{13} - 2 b_2 b_5 \varepsilon - 2 b_2 b_6 \varepsilon - b_7 \varepsilon - b_8 - b_2 b_9 - b_9 \mu \varepsilon, \\
&c_0 = b_1 b_2 b_3 b_4 [1 - \mathcal{R}_C] > 0 \text{ if } \mathcal{R}_C < 1.
\end{aligned}
\tag{13}
$$

It can be seen from and (13) that $c_3 > 0$ (since the entire model parameters are nonnegative). Furthermore, $c_0 > 0$ whenever $\mathcal{R}_C < 1$. Thus, the number of possible positive real roots the polynomial (12) can have depends on the signs of c_1, and c_2. This can be analyzed using the Descartes' rule of signs on the cubic $f(x) = c_3 x^3 + c_2 x^2 + c_1 x + c_0$ (with $= x = \lambda_C^*$). Hence, the following results are established.

Theorem 6: The COVID-19 mono-infection model (11) could have

(a). a unique endemic equilibrium point if $\mathcal{R}_C > 1$ either of the following holds.

   (i) $c_1 > 0$ and $c_2 > 0$.

   (ii) $c_1 < 0$ and $c_2 < 0$.

(b). more than one endemic equilibrium point if $\mathcal{R}_C > 1$ either of the following holds.

   (i) $c_1 > 0$ and $c_2 < 0$.

   (ii) $c_1 < 0$ and $c_2 > 0$.

(c). two endemic equilibrium points if $\mathcal{R}_C < 1$, $c_1 < 0$ and $c_2 < 0$.

Here, item (c) shows the happening of the backward bifurcation in the model (11) i.e., the locally asymptotically stable disease-free equilibrium point co-exists with a locally asymptotically stable endemic equilibrium point if $\mathcal{R}_C < 1$; examples of the existence of backward bifurcation phenomenon in mathematical epidemiological models, and the causes, can be seen in [8,17,26,31,58–60]. The epidemiological consequence is that the classical epidemiological requirement of having the reproduction number $\mathcal{R}_C$ to be less than one, even though necessary, is not sufficient for the effective control of the disease. The existence of the backward bifurcation phenomenon in sub-model (11) is now explored.

Theorem 7: The COVID-19 mono-infection model (11) exhibits backward bifurcation at $\mathcal{R}_C = 1$ whenever the inequality $D_2 > D_1$ holds, where

$D_1 = \frac{-\beta_2 \beta^* x_1^0 (\rho + \mu)(\mu + \eta) - \beta_2 \beta^* \varepsilon x_3^0 \rho (\mu + \eta) - \beta_2 \varepsilon \beta^* \varepsilon x_3^0 \mu (\mu + \eta)}{\mu (\rho + \mu)(\mu + \eta)}$ and $D_2 = \frac{\beta_2 \kappa \eta (\rho + \mu)}{\mu (\rho + \mu)(\mu + \eta)}$.

In this section, we have used the center manifold theory stated in [60] to ascertain the local asymptotic stability of the endemic equilibrium due to the convolution of the first approach (eigenvalues of the Jacobian). To make use of the center manifold theory, the following change of variables is made by symbolizing $S = x_1$, $C_p = x_2$, $C_v = x_3$, $C_i = x_4$ and $R = x_5$ such that $N_2 = x_1$

$+ x_2 + x_3 + x_4 + x_5$. Furthermore, by using vector notation $X = (x_1, x_2, x_3, x_4, x_5)^T$, the COVID-19 mono-infection model (11) can be written in the form $\frac{dX}{dt} = F(X)$ with $F = (f_1, f_2, f_3, f_4, f_5)^T$, as follows

$$
\begin{aligned}
\frac{dx_1}{dt} &= f_1 = k_1\Delta + \alpha_1 x_2 + \rho x_3 + \eta x_5 - \mu x_1 - \lambda_C x_1, \\
\frac{dx_2}{dt} &= f_2 = k_2\Delta - (\alpha_1 + \mu)x_2, \\
\frac{dx_3}{dt} &= f_4 = k_4\Delta - (\rho + \mu + \varepsilon\lambda_C)x_3, \\
\frac{dx_4}{dt} &= \lambda_C x_1 + \varepsilon\lambda_C x_3 - (\mu + d_1 + \kappa)x_4, \\
\frac{dx_5}{dt} &= \kappa x_4 - (\mu + \eta)x_5,
\end{aligned}
\tag{14}
$$

with $\lambda_C = \beta_2 x_4$ then the method entails evaluating the Jacobian of the system (14) at the DFE point E^0_{CM}, denoted by $J(E^0_{CM})$ and this gives us

$$
J(E^0_{CM}) = \begin{pmatrix}
-\mu & \alpha_2 & \rho & -\beta_2 x_1^0 & \eta \\
0 & -(\alpha_1 + \mu) & 0 & 0 & 0 \\
0 & 0 & -(\rho + \mu) & -\beta_2\varepsilon x_3^0 & 0 \\
0 & 0 & 0 & \beta_2 x_1^0 + \beta_2\varepsilon x_3^0 - (\mu + d_1 + \kappa) & 0 \\
0 & 0 & 0 & \kappa & -(\mu + \eta)
\end{pmatrix}.
$$

Consider, $\mathcal{R}_C = 1$ and suppose that $\beta_2 = \beta^*$ is chosen as a bifurcation parameter. From $\mathcal{R}_C = 1$ as $\mathcal{R}_C = \frac{\beta_2 x_2^0 + \varepsilon\beta_2 x_4^0}{\mu + d_1 + \kappa} = \frac{\beta_2 k_1\Delta(\alpha_1 + \mu)(\rho + \mu) + \beta_2\alpha_1 k_2\Delta(\rho + \mu) + \beta_2 k_4\Delta(\alpha_1 + \mu)(\rho + \mu\varepsilon)}{\mu(\alpha_1 + \mu)(\rho + \mu)(\mu + d_1 + \kappa)} = 1$.

Solving for β_2 we have got $\beta_2 = \beta^* = \frac{\mu(\alpha_1 + \mu)(\rho + \mu)(\mu + d_1 + \kappa))}{k_1\Delta(\alpha_1 + \mu)(\rho + \mu) + \alpha_1 k_2\Delta(\rho + \mu) + k_4\Delta(\alpha_1 + \mu)(\rho + \mu\varepsilon)}$.

$$
J_{\beta^*} = \begin{pmatrix}
-\mu & \alpha_2 & \rho & -\beta^* x_1^0 & \eta \\
0 & -(\alpha_1 + \mu) & 0 & 0 & 0 \\
0 & 0 & -(\rho + \mu) & -\beta^*\varepsilon x_3^0 & 0 \\
0 & 0 & 0 & \beta^* x_1^0 + \beta^*\varepsilon x_3^0 - (\mu + d_1 + \kappa) & 0 \\
0 & 0 & 0 & \kappa & -(\mu + \eta)
\end{pmatrix}.
$$

After some steps of the calculation we have determined the eigenvalues of J_{β^*} as $\lambda_1 = -\mu$, $\lambda_2 = -(\alpha_1 + \mu)$ or or $\lambda_3 = -(\rho + \mu)$ or $\lambda_4 = 0$ or $\lambda_5 = -(\mu + \eta)$. It follows that the Jacobian $J(E^0_{CM})$ of Eq (14) at the disease-free equilibrium with $\beta_2 = \beta^*$, denoted by J_{β^*}, has a simple zero eigenvalue with all the remaining eigenvalues have negative real part. Hence, Theorem 2 of Castillo-Chavez and Song stated in [60] can be used to analyze the dynamics of the model to show that the model (11) undergoes backward bifurcation at $\mathcal{R}_C = 1$.

Eigenvectors of J_{β^*}: For the case $\mathcal{R}_C = 1$, it can be shown that the Jacobian of the system (14) at $\beta_2 = \beta^*$ (denoted by J_{β^*}) has a right eigenvectors associated with the zero eigenvalue

given by $u = (u_1, u_2, u_3, u_4, u_5)^T$ as

$$
\begin{pmatrix}
-\mu & \alpha_2 & \rho & -\beta^* x_1^0 & \eta \\
0 & -(\alpha_1 + \mu) & 0 & 0 & 0 \\
0 & 0 & -(\rho + \mu) & -\beta^* \varepsilon x_3^0 & 0 \\
0 & 0 & 0 & \beta^* x_1^0 + \beta^* \varepsilon x_3^0 - (\mu + d_1 + \kappa) & 0 \\
0 & 0 & 0 & \kappa & -(\mu + \eta)
\end{pmatrix}
\begin{pmatrix}
u_1 \\ u_2 \\ u_3 \\ u_4 \\ u_5
\end{pmatrix}
=
\begin{pmatrix}
0 \\ 0 \\ 0 \\ 0 \\ 0
\end{pmatrix}. \quad (15)
$$

Then solving Eq (15) the right eigenvectors associated with the zero eigenvalue are given by

$$
u_1 = \frac{-\beta^* x_1^0 u_4 (\rho + \mu)(\mu + \eta) - \beta^* \varepsilon x_3^0 \rho (\mu + \eta) u_4 + \kappa \eta (\rho + \mu) u_4}{\mu (\rho + \mu)(\mu + \eta)},
$$

$$
u_2 = 0, \ u_3 = -\frac{\beta^* \varepsilon x_3^0}{(\rho + \mu)} u_4, \ u_4 = u_4 > 0, \ u_5 = \frac{\kappa}{\mu + \eta} u_4.
$$

Similarly, the left eigenvector associated with the zero eigenvalues at $\beta_2 = \beta^*$ given by $v = (v_1, v_2, v_3, v_4, v_5)^T$ as

$$
\begin{pmatrix} v_1 \\ v_2 \\ v_3 \\ v_4 \\ v_5 \end{pmatrix}^T
*
\begin{pmatrix}
-\mu & \alpha_2 & \rho & -\beta^* x_1^0 & \eta \\
0 & -(\alpha_1 + \mu) & 0 & 0 & 0 \\
0 & 0 & -(\rho + \mu) & -\beta^* \varepsilon x_3^0 & 0 \\
0 & 0 & 0 & D & 0 \\
0 & 0 & 0 & \kappa & -(\mu + \eta)
\end{pmatrix}
=
\begin{pmatrix}
0 \\ 0 \\ 0 \\ 0 \\ 0 \\ 0
\end{pmatrix}, \quad (16)
$$

where $D = \beta^* x_1^0 + \beta^* \varepsilon x_3^0 - (\mu + d_1 + \kappa)$.

Then solving Eq (16) the left eigenvectors associated with the zero eigenvalue are given by $v_1 = v_2 = v_3 = v_4 = 0$ and $v_4 = v_4 > 0$. After long steps of calculations the bifurcation coefficients a and b are obtained as

$$
a = \sum_{i,j,k=1}^{5} v_4 u_i u_j \left. \frac{\partial^2 f_4}{\partial x_i \partial x_j} \right. = 2 v_4 u_1 u_4 \left. \frac{\partial^2 f_4}{\partial x_1 \partial x_4} \right. + 2 v_4 u_3 u_4 \left. \frac{\partial^2 f_4}{\partial x_3 \partial x_4} \right.
$$

$$
= 2 v_4 u_4 \left[u_1 \left. \frac{\partial^2 f_4}{\partial x_1 \partial x_4} \right. + u_3 \left. \frac{\partial^2 f_4}{\partial x_3 \partial x_4} \right. \right], = 2 v_4 u_4 [\beta_2 u_1 + \beta_2 \varepsilon u_3]
$$

$$
= 2 v_4 u_4^2 \left[\frac{-\beta_2 \beta^* x_1^0 (\rho + \mu)(\mu + \eta) - \beta_2 \beta^* \varepsilon x_3^0 \rho (\mu + \eta) + \beta_2 \kappa \eta (\rho + \mu) - \beta_2 \varepsilon \beta^* \varepsilon x_3^0 \mu (\mu + \eta)}{\mu (\rho + \mu)(\mu + \eta)} \right],
$$

$$
= 2 v_4 u_4 [D_2 - D_1],
$$

where $D_1 = \frac{-\beta_2 \beta^* x_1^0 (\rho + \mu)(\mu + \eta) - \beta_2 \beta^* \varepsilon x_3^0 \rho (\mu + \eta) - \beta_2 \varepsilon \beta^* \varepsilon x_3^0 \mu (\mu + \eta)}{\mu (\rho + \mu)(\mu + \eta)}$, and $D_2 = \frac{\beta_2 \kappa \eta (\rho + \mu)}{\mu (\rho + \mu)(\mu + \eta)}$. Thus, the bifurcation coefficient a is positive whenever $D_2 > D_1$.

Moreover

$$
b = \sum_{i,k=1}^{5} v_k u_i \left. \frac{\partial^2 f_k}{\partial x_i \partial \beta} \right. (E_{CM}^0) = \sum_{i=1}^{5} v_4 u_i \left. \frac{\partial^2 f_4}{\partial x_i \partial \beta} \right. = v_4 u_4 \left. \frac{\partial^2 f_4}{\partial x_4 \partial \beta} \right.
$$

$$
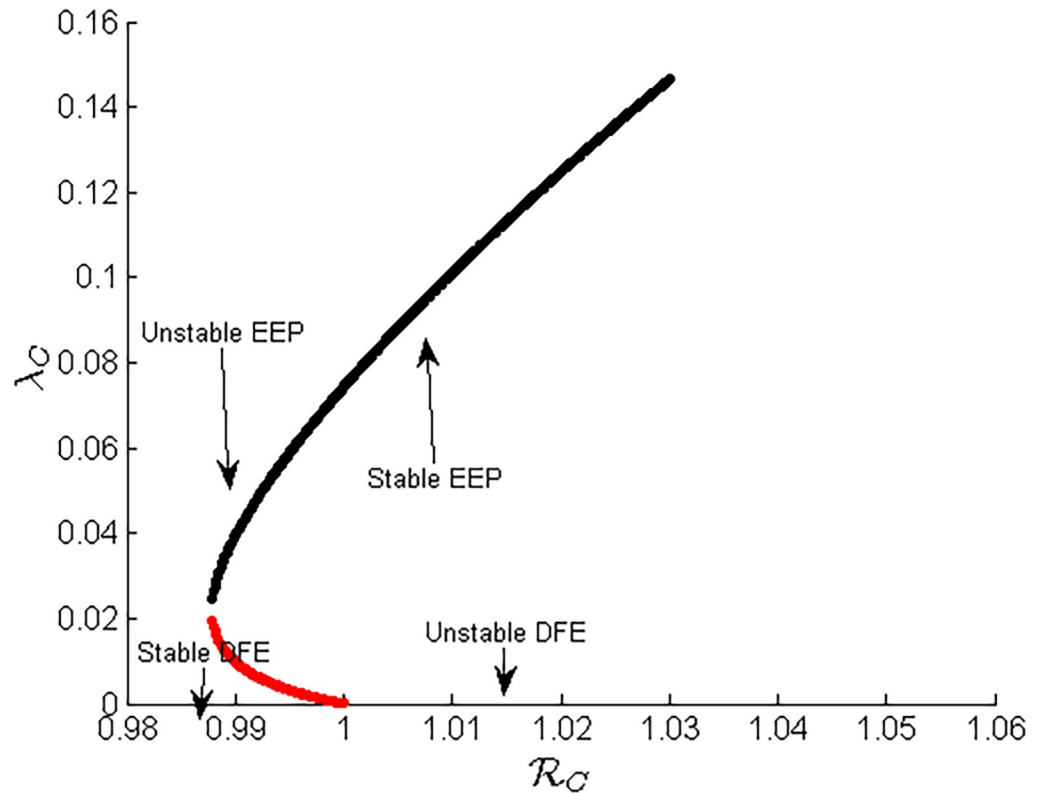= v_4 u_4 [x_1^0 u_1 + \varepsilon x_3^0 u_3] > 0.
$$

Fig 2. Backward bifurcation diagram.

Hence, from the theory of Castillo-Chavez and Song stated in [60] the COVID-19 mono-infection model (11) exhibits a phenomenon of backward bifurcation at $\mathcal{R}_C = 1$ and whenever $D_2 > D_1$.

The diagram representation of this bifurcation is given in Fig 2 below.

Fig 2 shows the appearance of backward bifurcation, which results in the coexistence of several equilibrium points. In such a case, the common conditions of disease eradication such as making $R_C < 1$ will not work, and the initial number of infected persons also plays a crucial role.

3.5. Analytical result of HIV/AIDS and COVID-19 co-infection model

3.5.1. Disease-free equilibrium point. The disease free equilibrium point of the dynamical system (3) when the state variable $C_i = H_u = H_a = M_u = M_a = 0$ is given by $E_0 =$

$$\left(S^0, \ C_q^0, \ H_p^0, C_v^0, \ C_i^0, \ H_u^0, H_p^0, \ M_u^0, \ M_a^0, R^0, \ H_t^0\right) =$$

$$\left(\frac{k_1\Delta}{\mu} + \frac{\alpha_1 k_2\Delta}{\alpha_1+\mu} + \frac{\alpha_2 k_3\Delta}{\alpha_2+\mu} + \frac{\rho k_4\Delta}{\rho+\mu}, \frac{k_2\Delta}{\alpha_1+\mu}, \frac{k_3\Delta}{\alpha_2+\mu}, \ \frac{k_4\Delta}{\rho+\mu}, 0, \ 0, \ 0, \ 0, \ 0, \ 0, \ 0\right).$$

3.5.2. Effective reproduction number of the co-infection model. The effective reproduction number of the dynamical system (3) by applying the next generation operator method is the largest (dominant) eigenvalue (spectral radius) of the matrix: $FV^{-1} = \left[\frac{\partial \mathcal{F}_i(E_0)}{\partial X_j}\right]\left[\frac{\partial v_i(E_0)}{\partial X_j}\right]$,

where $\mathcal{F}_i$ is the rate of appearance of new infection in compartment i, v_i is the transfer of infections from one compartment i to another, and E_0 is the disease-free equilibrium point. After

some steps of calculations we have determined that

$$
F = \begin{bmatrix}
\aleph_1 & 0 & \omega_1\aleph_1 & \omega_2\aleph_1 & 0 & 0 & 0 \\
0 & \aleph_2 & \rho_2\aleph_2 & \rho_3\aleph_2 & \rho_1\aleph_2 & 0 & 0 \\
0 & 0 & 0 & 0 & 0 & 0 & 0 \\
0 & 0 & 0 & 0 & 0 & 0 & 0 \\
0 & 0 & 0 & 0 & 0 & 0 & 0 \\
0 & 0 & 0 & 0 & 0 & 0 & 0 \\
0 & 0 & 0 & 0 & 0 & 0 & 0
\end{bmatrix},
$$

where $\aleph_1 = \beta_2 S + \beta_2 H_p + \varepsilon\beta_2 C_\nu$, $\aleph_2 = \frac{\beta_1}{N}\left(S + C_q + C_\nu\right)$, and

$$
V = \begin{bmatrix}
(\mu + d_1 + \kappa) & 0 & 0 & 0 & 0 & 0 & 0 \\
0 & (\theta + \mu + d_2) & -\theta_1 & 0 & 0 & 0 & 0 \\
0 & 0 & (\mu + d_4 + \delta + \theta_1) & 0 & 0 & 0 & 0 \\
0 & 0 & -\delta & (\mu + d_5 + \theta_2) & 0 & 0 & 0 \\
0 & -\theta & 0 & -\theta_2 & (\gamma + d_3 + \mu) & 0 & 0 \\
-\kappa & 0 & 0 & 0 & 0 & (\mu + \eta) & 0 \\
0 & 0 & 0 & 0 & -\gamma & 0 & \mu
\end{bmatrix}.
$$

Applying Mathematica we have determined as

$$
FV^{-1} = \begin{bmatrix}
\frac{\aleph_1}{(\mu + d_1 + \kappa)} & a_{21} & 0 & 0 & 0 & 0 & 0 \\
0 & \frac{\aleph_2}{(\theta + \mu + d_2)} + \frac{\rho_1\aleph_2\theta}{(\theta + \mu + d_2)(\gamma + d_3 + \mu)} & 0 & 0 & 0 & 0 & 0 \\
0 & a_{23} & 0 & 0 & 0 & 0 & 0 \\
0 & a_{24} & 0 & 0 & 0 & 0 & 0 \\
0 & a_{25} & 0 & 0 & 0 & 0 & 0 \\
0 & a_{26} & 0 & 0 & 0 & 0 & 0 \\
0 & a_{27} & 0 & 0 & 0 & 0 & 0
\end{bmatrix}.
$$

After some computations and simplifications we have determined the dominant eigenvalue in magnitude of the matrix FV^{-1} which is the HIV/AIDS and COVID-19 co-infection effective reproduction number given by

$$
\mathcal{R}_0^{HC} = \max\{\mathcal{R}_C, \mathcal{R}_{HM}\} = \max\{\frac{\beta_2 k_1\Delta(\alpha_1 + \mu)(\rho + \mu) + \beta_2\alpha_1 k_2\Delta(\rho + \mu) + \beta_2 k_4\Delta\rho(\alpha_1 + \mu) + \beta_2\varepsilon k_4\Delta\mu(\alpha_1 + \mu)}{\mu(\alpha_1 + \mu)(\rho + \mu)(\mu + d_1 + \kappa)}
$$

$$
,\frac{\beta_1(1 - k_3)(\alpha_2 + \mu) + \beta_1\alpha_2 k_3}{(\alpha_2 + \mu)(\theta + \mu + d_2)} + \frac{\beta_1\rho_1\theta(1 - k_3)(\alpha_2 + \mu) + \beta_1\rho_1\theta\alpha_2 k_3}{(\theta + \mu + d_2)(\gamma + \mu + d_3)}\},\text{where } \mathcal{R}_C =
$$

$\frac{\beta_2 S^0 + \varepsilon\beta_2 C_\nu^0}{\mu + d_1 + \kappa} = \frac{\beta_2 k_1\Delta(\alpha_1 + \mu)(\rho + \mu) + \beta_2\alpha_1 k_2\Delta(\rho + \mu) + \beta_2 k_4\Delta\rho(\alpha_1 + \mu) + \beta_2\varepsilon k_4\Delta\mu(\alpha_1 + \mu)}{\mu(\alpha_1 + \mu)(\rho + \mu)(\mu + d_1 + \kappa)}$ is the COVID-19 effective reproduction number and $\mathcal{R}_{HM} = \frac{\beta_1(1 - k_3)(\alpha_2 + \mu) + \beta_1\alpha_2 k_3}{(\alpha_2 + \mu)(\theta + \mu + d_2)} + \frac{\beta_1\rho_1\theta(1 - k_3)(\alpha_2 + \mu) + \beta_1\rho_1\theta\alpha_2 k_3}{(\theta + \mu + d_2)(\gamma + \mu + d_3)}$ is the HIV/AIDS effective reproduction number.

3.5.3. Locally asymptotically stability of the disease-free equilibrium point.

The Jacobian matrix of the system (3) at disease free equilibrium point is given as

$$J(E_0) = \begin{pmatrix}
-\mu & \alpha_1 & \alpha_2 & \rho & -\beta_2 A_1 & -\frac{\beta_1}{N}A_1 & -\frac{\beta_1}{N}A_1\rho_1 & -\aleph_4 & -\aleph_6 & \eta & 0 \\
0 & -(\alpha_1+\mu) & 0 & 0 & 0 & -\frac{\beta_1}{N}A_2 & -\frac{\beta_1}{N}A_2\rho_1 & -\frac{\beta_1}{N}A_2\rho_2 & -\frac{\beta_1}{N}A_2\rho_3 & 0 & 0 \\
0 & 0 & -(\alpha_2+\mu) & 0 & -\beta_2 A_3 & 0 & 0 & -\beta_2 A_3\omega_1 & -\beta_2 A_3\omega_2 & 0 & 0 \\
0 & 0 & 0 & -(\rho+\mu) & -\varepsilon\beta_2 A_4 & -\frac{\beta_1}{N}A_4 & -\frac{\beta_1}{N}A_4\rho_1 & -\aleph_5 & -\aleph_7 & 0 & 0 \\
0 & 0 & 0 & 0 & \aleph_3 & 0 & 0 & \omega_1\aleph_3 & \omega_2\aleph_3 & 0 & 0 \\
0 & 0 & 0 & 0 & 0 & \aleph_8 & \rho_1\aleph_8 & \rho_2\aleph_8+\theta_1 & \rho_3\aleph_8 & 0 & 0 \\
0 & 0 & 0 & 0 & 0 & \Theta & \aleph_9 & 0 & \theta_2 & 0 & 0 \\
0 & 0 & 0 & 0 & 0 & 0 & 0 & \aleph_{10} & 0 & 0 & 0 \\
0 & 0 & 0 & 0 & 0 & 0 & 0 & \delta & \aleph_{11} & 0 & 0 \\
0 & 0 & 0 & 0 & \kappa & 0 & 0 & 0 & 0 & -(\mu+\eta) & 0 \\
0 & 0 & 0 & 0 & 0 & 0 & \gamma & 0 & 0 & 0 & -\mu
\end{pmatrix},$$

where $\aleph_3 = \beta_2\left(S^0 + H_p + \varepsilon C_v\right) - (\mu+d_1+\kappa)$, $\aleph_4 = \left(\frac{\beta_1}{N}\rho_2 + \beta_2\omega_1\right)S^0$, $\aleph_5 = \left(\frac{\beta_1}{N}\rho_2 + \varepsilon\beta_2\omega_1\right)C_v$, $\aleph_6 = \left(\frac{\beta_1}{N}\rho_3 + \beta_2\omega_2\right)S^0$ and $\aleph_7 = \left(\frac{\beta_1}{N}\rho_3 + \varepsilon\beta_2\omega_2\right)C_v$, $\aleph_8 = \frac{\beta_1}{N}\left(S^0 + C_q + C_v\right) - (\theta+\mu+d_2)$, $\aleph_9 = -(\gamma+d_3+\mu)$, $\aleph_{10} = -(\mu+d_4+\delta+\theta_1)$, $\aleph_{11} = -(\mu+d_5+\theta_2)$.

Then the eigenvalues of the matrix $J(E_0)$ are $\lambda_1 = -\mu < 0$ or $\lambda_2 = -(\alpha_1+\mu) < 0$ or $\lambda_3 = -(\alpha_2+\mu) < 0$ or $\lambda_4 = -(\rho+\mu) < 0$ or $\lambda_5 = -\mu < 0$ or $\lambda_6 = -(\mu+\eta) < 0$ or $\lambda_7 = \frac{\beta_2\varepsilon k_4\Delta}{(\rho+\mu)(\mu+d_1+\kappa)}\left(\mathcal{R}_{CM}-1\right) < 0$ or $\lambda_8 = -(\mu+d_4+\delta+\theta_1) < 0$ or $\lambda_9 = -(\mu+d_5+\Theta_2) < 0$ or $\lambda^2 + [(\gamma+d_3+\mu) + (\theta+\mu+d_2) - \aleph_8]\lambda - [(\aleph_8 - (\theta+\mu+d_2))(\gamma+d_3+\mu) + \theta\rho_1\aleph_8] = 0$.

Then after some calculations we have got the last two eigenvalues of the quadratic equation as $\lambda_{10} < 0$ and $\lambda_{11} < 0$ whenever $\mathcal{R}_0^{HC} = \max\{\mathcal{R}_C, \mathcal{R}_{HM}\} < 1$. Thus, since all the eigenvalues are negative, the disease-free equilibrium point of the full model (3) is locally asymptotically stable whenever $\mathcal{R}_0^{HC} = \max\{\mathcal{R}_C, \mathcal{R}_{HM}\} < 1$.

3.5.4. Global asymptotic stability of disease-free equilibrium point.

In this sub-section we have used the method derived by Castillo-Chavez et al. and stated in reference [61] to look into the global asymptotic stability (GAS) of the co-infection model (3) disease-free equilibrium point. We mention two requirements that, if satisfied, also ensure the disease-free equilibrium is globally asymptotically stable. Then the new system (3) is rewritten as:

$$\frac{d\Psi}{dt} = F(\Psi, Y),$$

$$\frac{dY}{dt} = G(\Psi, Y), \quad G(\Psi, 0) = 0,$$

where $\Psi = (S, C_q, H_p, C_v) \in \mathbb{R}^4$ denotes the number of uninfected components and $z =$

$(C_i,\ H_u,\ H_a, M_u,\ M_a,\ R,\ H_t) \in \mathbb{R}^7$ denotes the number of infected components. $\Pi_0 = (\Psi_0, 0)$, denotes the disease-free equilibrium point of the system. The following requirements must be satisfied to ensure the globally asymptotic stability:

(H_1) For $\frac{d\Psi}{dt} = F(\Psi, 0)$, Π_0 is globally asymptotically stable.

(H_2) $G(\Psi, Y) = AY - \widehat{G}(\Psi, Y)$, $\widehat{G}(\Psi, Y) \geq 0$, for $(\Psi, Y) \in \Omega$, where $A = D_Y G(\Psi_0, 0)$ is a Metzler matrix (the off diagonal elements of A are nonnegative) and Ω is the region where the model makes biological sense.

Theorem 8: The fixed point $\Pi_0 = (\Psi_0, 0)$ is a globally asymptotically stable equilibrium point of system (3) provided $\mathcal{R}_0^{HC} < 1$ and the assumptions (H_1) and (H_2) are satisfied otherwise unstable.

Proof: The system (1) is rewritten as

$$\frac{d\Psi}{dt} = F(\Psi, Y) = \begin{pmatrix} k_1\Delta + \alpha_1 C_q + \alpha_2 H_p + \rho C_v + \eta R - (\lambda_H + \lambda_C + \mu)S \\ k_2\Delta - (\lambda_H + \alpha_1 + \mu)C_q \\ k_3\Delta - (\alpha_2 + \mu + \lambda_C)H_p \\ k_4\Delta - (\rho + \mu + \lambda_H + \varepsilon\lambda_C)C_v \end{pmatrix},$$

$$F(\Psi, 0) = \begin{pmatrix} k_1\Delta + \alpha_1 C_q + \alpha_2 H_p + \rho C_v - \mu S \\ k_2\Delta - (\alpha_1 + \mu)C_q \\ k_3\Delta - (\alpha_2 + \mu)H_p \\ k_4\Delta - (\rho + \mu)C_v \end{pmatrix},$$

where Ψ represents the number of non-infectious compartments and Y represents the number of infectious compartments.

And

$$G(\Psi, Y) = \begin{pmatrix} \lambda_C S + \lambda_C H_P + \varepsilon\lambda_C C_v - (\mu + d_1 + \kappa + \upsilon\lambda_H)C_i \\ \lambda_H S + \lambda_H C_q + \lambda_H C_v + \theta_1 M_u - (\theta + \mu + d_2 + \phi_1\lambda_C)H_u \\ \theta H_u + \theta_2 M_a + \theta_3 M_u - (\gamma + d_3 + \mu + \phi_2\lambda_C)H_a \\ \phi_1\lambda_C H_u + \upsilon\lambda_H C_i - (\mu + \theta_3 + d_4 + \delta + \Theta_1)M_u \\ \delta M_u + \phi_2\lambda_C H_a - (\mu + d_5 + \theta_2)M_a \\ \kappa C_i - (\mu + \eta)R \\ \gamma H_a - \mu H_t \end{pmatrix}.$$

Then $G(\Psi, Y) = AY - \widehat{G}(\Psi, Y)$, where,

$$A = \begin{pmatrix} \Sigma_1 & 0 & 0 & \beta_2\omega_1(S + H_P + \varepsilon C_v) & \beta_2\omega_2(S + H_P + \varepsilon C_v) & 0 & 0 \\ 0 & \Sigma_2 & \Sigma_3 & \frac{\beta_1\rho_2}{N}\left(S + C_q + C_v\right) + \theta_1 & \frac{\beta_1\rho_3}{N}\left(S + C_q + C_v\right) & 0 & 0 \\ 0 & \theta & \Sigma_4 & \theta_3 & \theta_2 & 0 & 0 \\ 0 & 0 & 0 & -(\mu + \theta_3 + d_4 + \delta + \Theta_1) & 0 & 0 & 0 \\ 0 & 0 & 0 & \delta & -(\mu + d_5 + \theta_2) & 0 & 0 \\ \kappa & 0 & 0 & 0 & 0 & -(\mu + \eta) & 0 \\ 0 & 0 & \gamma & 0 & 0 & 0 & -\mu \end{pmatrix},$$

where $\Sigma_1 = \beta_2(S + H_P + \varepsilon C_v) - (\mu + d_1 + \kappa)$, $\Sigma_2 = \frac{\beta_1}{N}\left(S + C_q + C_v\right) - (\theta + \mu + d_2)$, $\Sigma_3 = \frac{\beta_1\rho_1}{N}\left(S + C_q + C_v\right)$ and $\Sigma_4 = -(\gamma + d_3 + \mu)$, so that

$$AY = \begin{pmatrix} \lambda_C(S + H_P + \varepsilon C_v) - (\mu + d_1 + \kappa)C_i \\ -(\theta + \mu + d_2)H_u + \lambda_H\left(S + C_q + C_v\right) + \theta_1 M_u \\ \theta H_u - (\gamma + d_3 + \mu)H_a + \theta_3 M_u + \theta_2 M_a \\ -(\mu + \theta_3 + d_4 + \delta + \Theta_1)M_u \\ \delta M_u - (\mu + d_5 + \theta_2)M_a \\ \kappa C_i - (\mu + \eta)R \\ \gamma H_a - \mu H_t \end{pmatrix}.$$

We have determined that,

$$\widehat{G}(\Psi, Y) = \begin{pmatrix} \lambda_C\frac{\Delta}{\mu}\left(k_1 + \frac{\alpha_1 k_2\mu}{\alpha_1 + \mu} + \frac{(\alpha_2 + 1)k_3\mu}{\alpha_2 + \mu} + \frac{(\rho + 1)k_4\mu}{\rho + \mu}\right) - \lambda_C\left(S + C_q + \varepsilon C_v\right) + \upsilon\lambda_H C_i \\ \lambda_H\frac{\Delta}{\mu}\left(k_1 + \frac{k_2\mu(\alpha_1 + 1)}{\alpha_1 + \mu} + \frac{\alpha_2 k_3\mu}{\alpha_2 + \mu} + \frac{k_4\mu(\rho + 1)}{\rho + \mu}\right) - \lambda_H\left(S + C_q + C_v\right) + \phi_1\lambda_C H_u \\ \phi_2\lambda_C H_a \\ -\phi_1\lambda_C H_u - \upsilon\lambda_H C_i \\ -\phi_2\lambda_C H_a \\ 0 \\ 0 \end{pmatrix}.$$

It is clear from the above discussion, that, $\widehat{G}(\Psi, Y) \ngeq 0$. Hence by the same reason given by results in reference [38], the disease-free equilibrium point may not be globally asymptotically stable.

4. Analysis of the optimal control strategy

In this section, we provide a thorough qualitative analysis of the time-dependent HIV/AIDS and COVID-19 co-infection model (3). The Pontryagin's Maximum Principle stated in literatures [25,43,51,52,55] is used to describe this analysis, with the aim of minimizing the HIV/AIDS infection aware individuals denoted by H_a, the COVID-19 infected individuals denoted by C_i and the total HIV/AIDS and COVID-19 co-infected individuals denoted by $M_u + M_a$. In the case of time-dependent optimal control, we employ Pontryagin's Maximum Principle to derive the necessary conditions for diseases control mechanisms. After incorporating the controls into the HIV/AIDS and COVID-19 co-infection transmission model (3), the optimal control problem is as follows:

$$\dot{S} = k_1\Delta + \alpha_1 C_q + \alpha_2 H_p + \rho C_v + \eta R - (1 - \mathfrak{u}_1)\lambda_H S - (1 - \mathfrak{u}_2)\lambda_C S - \mu S,$$

$$\dot{C}_q = k_2\Delta - (1 - \mathfrak{u}_1)\lambda_H C_q - (\alpha_1 + \mu)C_q,$$

$$\dot{H}_p = k_3\Delta - (1 - \mathfrak{u}_2)\lambda_C H_p - (\alpha_2 + \mu)H_p,$$

$$\dot{C}_v = k_4\Delta - (1 - \mathfrak{u}_1)\lambda_H C_v - (1 - \mathfrak{u}_2)\varepsilon\lambda_C C_v - (\rho + \mu)C_v,$$

$$\dot{C}_i = (1 - \mathfrak{u}_2)\lambda_C S + (1 - \mathfrak{u}_2)\lambda_C H_p + (1 - \mathfrak{u}_2)\varepsilon\lambda_C C_v - (1 - \mathfrak{u}_1)\upsilon\lambda_H C_i - (\mu + d_1 + \mathfrak{u}_3\kappa)C_i,$$

$$\dot{H}_u = (1 - \mathfrak{u}_1)\lambda_H S + (1 - \mathfrak{u}_1)\lambda_H C_q + (1 - \mathfrak{u}_1)\lambda_H C_v + \mathfrak{u}_3\theta_1 M_u - (1 - \mathfrak{u}_2)\phi_1\lambda_C H_u - (\theta + \mu + d_2)H_u, \quad (17)$$

$$\dot{H}_a = \theta H_u + \mathfrak{u}_3\theta_2 M_a - (1 - \mathfrak{u}_2)\phi_2\lambda_C H_a - (\mathfrak{u}_4\gamma + d_3 + \mu)H_a,$$

$$\dot{M}_u = (1 - \mathfrak{u}_2)\phi_1\lambda_C H_u + (1 - \mathfrak{u}_1)\upsilon\lambda_H H_p - (\mu + d_4 + \delta + \mathfrak{u}_3\theta_1)M_u,$$

$$\dot{M}_a = \delta M_u + (1 - \mathfrak{u}_2)\phi_2\lambda_C H_p - (\mu + d_5 + \mathfrak{u}_3\theta_2)M_a,$$

$$\dot{R} = \mathfrak{u}_3\kappa A_5 - (\mu + \eta)R,$$

$$\dot{H}_t = \mathfrak{u}_4\gamma H_p - \mu H_t,$$

with the corresponding initial conditions

$$S(0) > 0, C_q(0) \geq 0, H_p(0) \geq 0, C_v(0) \geq 0, C_i(0) \geq 0, H_u(0) \geq 0, H_a(0) \geq 0, M_u(0)$$
$$\geq 0, M_a(0) \geq 0, R(0) > 0, \text{ and } H_t(0) > 0, \quad (18)$$

and $0 \leq \mathfrak{u}_1(t) \leq 1$ represents HIV/AIDS infection protective control, $0 \leq \mathfrak{u}_2(t) \leq 1$ represents the COVID-19 infections protective control using quarantine, $0 \leq \mathfrak{u}_3(t) \leq 1$ represents the COVID-19 infection treatment control, and $0 \leq \mathfrak{u}_4(t) \leq 1$ represents the HIV/AIDS treatment control.

The objective is to find the optimal control values $\mathfrak{u}^* = \left(\mathfrak{u}_1^*, \mathfrak{u}_2^*, \mathfrak{u}_3^*, \mathfrak{u}_4^*\right)$ of the controls $\mathfrak{u} = (\mathfrak{u}_1, \mathfrak{u}_2, \mathfrak{u}_3, \mathfrak{u}_4)$ such that the associated state trajectories $\left(S^*, C_q^*, H_p^*, C_v^*, C_i^*, H_u^*, H_p^*, M_u^*, M_a^*, R^*, H_t^*\right)$ are solution of the optimal control system (17) in the intervention time interval $[0, T_f]$ with initial conditions as given in (18) and minimize

the objective functional given by

$$J(u_1, u_2, u_3, u_4)$$
$$= \int_0^{T_f} \left(w_1 C_i + w_2 H_p + w_3 M_u + w_4 M_a + \frac{\mathcal{B}_1}{2} u_1^2 + \frac{\mathcal{B}_2}{2} u_2^2 + \frac{\mathcal{B}_3}{2} u_3^2 + \frac{\mathcal{B}_4}{2} u_4^2 \right) dt, \quad (19)$$

where the coefficients $w_1, w_2, w_3,$
and w_4 are positive weight constants and $\frac{\mathcal{B}_1}{2}, \frac{\mathcal{B}_2}{2}, \frac{\mathcal{B}_3}{2}$ and $\frac{\mathcal{B}_4}{2}$ are the measure of relative costs of interventions associated with the controls u_1, u_2, u_3 and u_4, respectively, and also balances the units of integrand. In the cost functional, the term $w_1 A_5$ refer to the cost related to COVID-19 infected class, the term $w_2 H_u$ refer to the cost related to individuals mono-infected with HIV and aware, the term $w_3 A_8$ refer to the cost related to co-infected individuals unaware of HIV infection and the term $w_4 M_a$ refer to the cost related to co-infected individuals aware of HIV infection.

$$I\left(S, C_q, H_p, C_v, C_i, H_u, H_a, M_u, M_a, R, H_t, u\right) = w_1, C_i + w_2 H_a + w_3 M_u + w_4 M_a +$$
$\frac{\mathcal{B}_1}{2} u_1^2 + \frac{\mathcal{B}_2}{2} u_2^2 + \frac{\mathcal{B}_3}{2} u_3^2 + \frac{\mathcal{B}_4}{2} u_4^2$, measures the current cost at time t. The set of admissible Lebesgue measurable control functions is defined by

$$\Omega_u = \left\{ (u_1(t), u_2(t), u_3(t), u_4(t)) \in L^4 : 0 \le u_1(t), u_2(t), u_3(t), u_4(t) \le 1, t \in \left[0, T_f\right] \right\}. \quad (20)$$

More precisely, we seek an optimal control pair

$$J\left(u_1^*, u_2^*, u_3^*, u_4^*\right) = \min_{\Omega_u} J(u_1, u_2, u_3, u_4). \quad (21)$$

Theorem 9 (Existence Theorem): There exists an optimal control $u^* = \left(u_1^*, u_2^*, u_3^*, u_4^*\right)$ in Ω_u and a corresponding solution vector $\left(S^*, C_q^*, H_p^*, C_v^*, C_i^*, H_u^*, H_a^*, M_u^*, M_a^*, R^*, H_t^*\right)$ to the optimal control dynamical system (17) with the initial values (18) such that $J\left(u_1^*, u_2^*, u_3^*, u_4^*\right) = \min_{\Omega_u} J(u_1, u_2, u_3, u_4)$.

Note: We utilize Pontryagin's Maximal principle stated in literatures [51,52,55], to determine the prerequisites for the optimal control model (17). The optimal control problem (17) and (19) defined Hamiltonian (H) function is expressed as

$$\mathcal{H} = w_1 C_i + w_2 H_a + w_3 M_u + w_4 M_a + \frac{\mathcal{B}_1}{2} u_1^2 + \frac{\mathcal{B}_2}{2} u_2^2 + \frac{\mathcal{B}_3}{2} u_3^2 + \frac{\mathcal{B}_4}{2} u_4^2 + \sum_{i=1}^{11} \lambda_i \mathcal{G}_i, \quad (22)$$

where $\mathcal{G}_i$ stands for the ith state variable equation and $\lambda_1(t), \lambda_2(t), \lambda_3(t), \lambda_4(t), \lambda_5(t), \lambda_6(t), \lambda_7(t), \lambda_8(t), \lambda_9(t), \lambda_{10}(t)$ and $\lambda_{11}(t)$ are adjoint variables. Similarly to obtain the co-state variables by using Pontryagin's Maximum Principle stated in literatures [51,52,55], with the existence result the following theorem is stated:

Theorem 10: Let $u^* = \left(u_1^*, u_2^*, u_3^*, u_4^*\right)$ be the optimal control and $S^*, C_q^*, H_p^*, C_v^*, C_i^*, H_u^*, H_a^*, M_u^*, M_a^*, R^*, H_t^*$ be the associated unique optimal solutions of the optimal control problem (17) with initial condition (18) and objective functional (19) with fixed final time T_f (20). Then there exists adjoint function $\lambda_i^*(\cdot), i = 1, \ldots, 11$ satisfying the

following canonical equations

$$\frac{d\lambda_1}{dt} = (1 - \mathfrak{u}_1)\lambda_H^*(\lambda_1 - \lambda_6) + (1 - \mathfrak{u}_2)\lambda_C^*(\lambda_1 - \lambda_5) + \mu\lambda_1,$$

$$\frac{d\lambda_2}{dt} = (1 - \mathfrak{u}_1)\lambda_H^*(\lambda_2 - \lambda_6) + \alpha_1(\lambda_2 - \lambda_1) + \mu\lambda_2,$$

$$\frac{d\lambda_3}{dt} = (1 - \mathfrak{u}_2)\lambda_C^*(\lambda_3 - \lambda_5) + \alpha_2(\lambda_3 - \lambda_1) + \mu\lambda_3,$$

$$\frac{d\lambda_4}{dt} = (1 - \mathfrak{u}_1)\lambda_H^*(\lambda_4 - \lambda_6) + (1 - \mathfrak{u}_2)\varepsilon\lambda_C^*(\lambda_4 - \lambda_5) + \rho(\lambda_4 - \lambda_1) + \mu\lambda_4,$$

$$\frac{d\lambda_5}{dt} = -\mathfrak{w}_1 + (1 - \mathfrak{u}_2)\beta_2 A_1^*(\lambda_1 - \lambda_5) + (1 - \mathfrak{u}_2)\beta_2 A_3^*(\lambda_3 - \lambda_5) + (1 - \mathfrak{u}_2)\varepsilon\beta_2 A_4^*(\lambda_4 - \lambda_5) +$$

$$\qquad (1 - \mathfrak{u}_2)\phi_1\beta_2 A_6^*(\lambda_6 - \lambda_8) + (1 - \mathfrak{u}_2)\phi_2\beta_2 A_7^*(\lambda_7 - \lambda_9) + (1 - \mathfrak{u}_1)\upsilon\lambda_H(\lambda_5 - \lambda_8) + (\mu + d_1)\lambda_5 + \mathfrak{u}_3\kappa(\lambda_5 - \lambda_{10}),$$

$$\frac{d\lambda_6}{dt} = (1 - \mathfrak{u}_1)\frac{\beta_1}{N}A_1^*(\lambda_1 - \lambda_6) + (1 - \mathfrak{u}_1)\frac{\beta_1}{N}A_2^*(\lambda_2 - \lambda_6) + (1 - \mathfrak{u}_1)\frac{\beta_1}{N}A_4^*(\lambda_4 - \lambda_6) +$$

$$\qquad (1 - \mathfrak{u}_1)\upsilon\frac{\beta_1}{N}A_5^*(\lambda_5 - \lambda_8) + (1 - \mathfrak{u}_2)\phi_1\lambda_C^*(\lambda_6 - \lambda_8) + (\mu + d_2)\lambda_6 + \Theta(\lambda_6 - \lambda_7),$$

$$\frac{d\lambda_7}{dt} = -\mathfrak{w}_2 + (1 - \mathfrak{u}_1)\frac{\beta_1\rho_1}{N}A_1^*(\lambda_1 - \lambda_6) + (1 - \mathfrak{u}_1)\frac{\beta_1\rho_1}{N}A_2^*(\lambda_2 - \lambda_6) + (1 - \mathfrak{u}_1)\frac{\beta_1\rho_1}{N}A_4^*(\lambda_4 - \lambda_6) +$$

$$\qquad (1 - \mathfrak{u}_1)\upsilon\frac{\beta_1\rho_1}{N}A_5^*(\lambda_5 - \lambda_8) + (1 - \mathfrak{u}_2)\phi_2\lambda_C^*(\lambda_7 - \lambda_9) + (d_3 + \mu)\lambda_7 + \mathfrak{u}_4\gamma(\lambda_7 - \lambda_{11}),$$

$$\frac{d\lambda_8}{dt} = -\mathfrak{w}_3 + (1 - \mathfrak{u}_1)\frac{\beta_1\rho_2}{N}A_1^*(\lambda_1 - \lambda_6) + (1 - \mathfrak{u}_2)\beta_2\omega_1 A_1^*(\lambda_1 - \lambda_5) + (1 - \mathfrak{u}_1)\frac{\beta_1\rho_2}{N}A_2^*(\lambda_2 - \lambda_6) + (1 - \mathfrak{u}_2)$$

$$\qquad \beta_2\omega_1 A_3^*(\lambda_3 - \lambda_5) + (1 - \mathfrak{u}_1)\frac{\beta_1\rho_2}{N}A_4^*(\lambda_4 - \lambda_6) + (1 - \mathfrak{u}_2)\varepsilon\beta_2\omega_1 A_4^*(\lambda_4 - \lambda_5) + (1 - \mathfrak{u}_1)\upsilon\frac{\beta_1\rho_2}{N}A_5^*(\lambda_5 - \lambda_8) + \mathfrak{u}_3\theta_1$$

$$\qquad (\lambda_8 - \lambda_6) + (1 - \mathfrak{u}_2)\phi_1\beta_2\omega_1 A_6^*(\lambda_6 - \lambda_8) + (1 - \mathfrak{u}_2)\phi_2\beta_2\omega_1 A_7^*(\lambda_7 - \lambda_9) + (\mu + d_4)\lambda_8 + \delta(\lambda_8 - \lambda_9),$$

$$\frac{d\lambda_9}{dt} = -\mathfrak{w}_4 + (1 - \mathfrak{u}_1)\frac{\beta_1\rho_3}{N}A_1^*(\lambda_1 - \lambda_6) + (1 - \mathfrak{u}_2)\beta_2\omega_2 A_1^*(\lambda_1 - \lambda_5) + (1 - \mathfrak{u}_1)\frac{\beta_1\rho_3}{N}A_2^*(\lambda_2 - \lambda_6) + (1 - \mathfrak{u}_2)\beta_2\omega_2 A_3^*$$

$$\qquad (\lambda_3 - \lambda_5) + (1 - \mathfrak{u}_1)\frac{\beta_1\rho_3}{N}A_4^*(\lambda_4 - \lambda_6) + (1 - \mathfrak{u}_2)\varepsilon\beta_2\omega_2 A_4^*(\lambda_4 - \lambda_5) + (1 - \mathfrak{u}_1)\upsilon\frac{\beta_1\rho_3}{N}A_5^*(\lambda_5 - \lambda_8) +$$

$$\qquad (1 - \mathfrak{u}_2)\phi_1\beta_2\omega_2 A_6^*(\lambda_6 - \lambda_8) + \mathfrak{u}_3\theta_2(\lambda_9 - \lambda_7) + (1 - \mathfrak{u}_2)\phi_2\beta_2\omega_2 A_7^*(\lambda_7 - \lambda_9) + (\mu + d_5)\lambda_9,$$

$$\frac{d\lambda_{10}}{dt} = -\eta\lambda_1 + (\mu + \eta)\lambda_{10},$$

$$\frac{d\lambda_{11}}{dt} = \mu\lambda_{11},$$

$$(23)$$

with transiversality conditions

$$\lambda_i^*\left(T_f\right) = 0, \ i = 1, \ 2, \ \ldots, 11. \tag{24}$$

Moreover, the corresponding optimal controls $\mathfrak{u}_1^*(t)$, $\mathfrak{u}_2^*(t)$, $\mathfrak{u}_3^*(t)$, and $\mathfrak{u}_4^*(t)$ are given by

$$\mathfrak{u}_1^*(t) = \max\left\{0, \min\left\{\frac{\lambda_H^* S^*(\lambda_6 - \lambda_1) + \lambda_H^* C_q^*(\lambda_6 - \lambda_2) + \lambda_H^* C_v^*(\lambda_6 - \lambda_4) + \upsilon\lambda_H^* C_i^*(\lambda_8 - \lambda_5)}{\mathfrak{B}_1}, 1\right\}\right\},$$

$$\mathfrak{u}_2^*(t) = \max\left\{0, \min\left\{\frac{\lambda_C^* S^*(\lambda_5 - \lambda_1) + \lambda_C^* H_p^*(\lambda_5 - \lambda_3) + \varepsilon\lambda_C^* C_v^*(\lambda_5 - \lambda_4) + \phi_1\lambda_C^* H_u^*(\lambda_8 - \lambda_6) + \phi_2\lambda_C^* H_p^*(\lambda_9 - \lambda_7)}{\mathfrak{B}_2}, 1\right\}\right\}, \tag{25}$$

$$\mathfrak{u}_3^*(t) = \max\left\{0, \min\left\{\frac{\Theta_1 M_u^*(\lambda_8 - \lambda_6) + \Theta_2 M_a^*(\lambda_9 - \lambda_7) + \kappa C_i^*(\lambda_5 - \lambda_{10})}{\mathfrak{B}_3}, 1\right\}\right\},$$

$$\mathfrak{u}_4^*(t) = \max\left\{0, \min\left\{\frac{\gamma H_p^*(\lambda_7 - \lambda_{11})}{\mathfrak{B}_4}, 1\right\}\right\}.$$

Proof: To obtain the form of the co-state equations we compute the derivative of the Hamiltonian function ($\mathcal{H}$), given in (22), with respect to S^*, C_q^*, H_p^*, C_v^*, C_i^*, H_u^*, H_a^*, M_u^*, M_a^*, R^* and H_t^* respectively. Then the adjoint or co-state equations obtained are given by:

$$\frac{d\lambda_1}{dt} = -\frac{\partial \mathcal{H}}{\partial S} = (1-u_1)\lambda_H^*(\lambda_1 - \lambda_6) + (1-u_2)\lambda_C^*(\lambda_1 - \lambda_5) + \mu\lambda_1,$$

$$\frac{d\lambda_2}{dt} = -\frac{\partial \mathcal{H}}{\partial C_q} = (1-u_1)\lambda_H^*(\lambda_2 - \lambda_6) + \alpha_1(\lambda_2 - \lambda_1) + \mu\lambda_2,$$

$$\frac{d\lambda_3}{dt} = -\frac{\partial \mathcal{H}}{\partial H_p} = (1-u_2)\lambda_C^*(\lambda_3 - \lambda_5) + \alpha_2(\lambda_3 - \lambda_1) + \mu\lambda_3,$$

$$\frac{d\lambda_4}{dt} = -\frac{\partial \mathcal{H}}{\partial C_v} = (1-u_1)\lambda_H^*(\lambda_4 - \lambda_6) + (1-u_2)\varepsilon\lambda_C^*(\lambda_4 - \lambda_5) + \rho(\lambda_4 - \lambda_1) + \mu\lambda_4,$$

$$\frac{d\lambda_5}{dt} = -\frac{\partial \mathcal{H}}{\partial C_i} = -\mathfrak{w}_1 + (1-u_2)\beta_2 A_1^*(\lambda_1 - \lambda_5) + (1-u_2)\beta_2 A_3^*(\lambda_3 - \lambda_5) + (1-u_2)\varepsilon\beta_2 A_4^*(\lambda_4 - \lambda_5) +$$

$$(1-u_2)\phi_1\beta_2 A_6^*(\lambda_6 - \lambda_8) + (1-u_2)\phi_2\beta_2 A_7^*(\lambda_7 - \lambda_9) + (1-u_1)\upsilon\lambda_H(\lambda_5 - \lambda_8) + (\mu + d_1)\lambda_5 + u_3\kappa(\lambda_5 - \lambda_{10}),$$

$$\frac{d\lambda_6}{dt} = -\frac{\partial \mathcal{H}}{\partial H_u} = (1-u_1)\frac{\beta_1}{N}A_1^*(\lambda_1 - \lambda_6) + (1-u_1)\frac{\beta_1}{N}A_2^*(\lambda_2 - \lambda_6) + (1-u_1)\frac{\beta_1}{N}A_4^*(\lambda_4 - \lambda_6) +$$

$$(1-u_1)\upsilon\frac{\beta_1}{N}A_5^*(\lambda_5 - \lambda_8) + (1-u_2)\phi_1\lambda_C^*(\lambda_6 - \lambda_8) + (\mu + d_2)\lambda_6 + \Theta(\lambda_6 - \lambda_7),$$

$$\frac{d\lambda_7}{dt} = -\frac{\partial \mathcal{H}}{\partial H_a} = -\mathfrak{w}_2 + (1-u_1)\frac{\beta_1\rho_1}{N}A_1^*(\lambda_1 - \lambda_6) + (1-u_1)\frac{\beta_1\rho_1}{N}A_2^*(\lambda_2 - \lambda_6) + (1-u_1)\frac{\beta_1\rho_1}{N}A_4^*(\lambda_4 - \lambda_6) +$$

$$(1-u_1)\upsilon\frac{\beta_1\rho_1}{N}A_5^*(\lambda_5 - \lambda_8) + (1-u_2)\phi_2\lambda_C^*(\lambda_7 - \lambda_9) + (d_3 + \mu)\lambda_7 + u_4\gamma(\lambda_7 - \lambda_{11}),$$

$$\frac{d\lambda_8}{dt} = -\frac{\partial \mathcal{H}}{\partial M_u} = -\mathfrak{w}_3 + (1-u_1)\frac{\beta_1\rho_2}{N}A_1^*(\lambda_1 - \lambda_6) + (1-u_2)\beta_2\omega_1 A_1^*(\lambda_1 - \lambda_5) + (1-u_1)\frac{\beta_1\rho_2}{N}A_2^*(\lambda_2 - \lambda_6) +$$

$$(1-u_2)\beta_2\omega_1 A_3^*(\lambda_3 - \lambda_5) + (1-u_1)\frac{\beta_1\rho_2}{N}A_4^*(\lambda_4 - \lambda_6) + (1-u_2)\varepsilon\beta_2\omega_1 A_4^*(\lambda_4 - \lambda_5) + (1-u_1)\upsilon\frac{\beta_1\rho_2}{N}A_5^*$$

$$(\lambda_5 - \lambda_8) + u_3\theta_1(\lambda_8 - \lambda_6) + (1-u_2)\phi_1\beta_2\omega_1 A_6^*(\lambda_6 - \lambda_8) + (1-u_2)\phi_2\beta_2\omega_1 A_7^*(\lambda_7 - \lambda_9) + (\mu + d_4)\lambda_8 + \delta(\lambda_8 - \lambda_9),$$

$$\frac{d\lambda_9}{dt} = -\frac{\partial \mathcal{H}}{\partial M_a} = -\mathfrak{w}_4 + (1-u_1)\frac{\beta_1\rho_3}{N}A_1^*(\lambda_1 - \lambda_6) + (1-u_2)\beta_2\omega_2 A_1^*(\lambda_1 - \lambda_5) + (1-u_1)\frac{\beta_1\rho_3}{N}A_2^*(\lambda_2 - \lambda_6) +$$

$$(1-u_2)\beta_2\omega_2 A_3^*(\lambda_3 - \lambda_5) + (1-u_1)\frac{\beta_1\rho_3}{N}A_4^*(\lambda_4 - \lambda_6) + (1-u_2)\varepsilon\beta_2\omega_2 A_4^*(\lambda_4 - \lambda_5) + (1-u_1)\upsilon\frac{\beta_1\rho_3}{N}A_5^*(\lambda_5 - \lambda_8) +$$

$$(1-u_2)\phi_1\beta_2\omega_2 A_6^*(\lambda_6 - \lambda_8) + u_3\theta_2(\lambda_9 - \lambda_7) + (1-u_2)\phi_2\beta_2\omega_2 A_7^*(\lambda_7 - \lambda_9) + (\mu + d_5)\lambda_9,$$

$$\frac{d\lambda_{10}}{dt} = -\frac{\partial \mathcal{H}}{\partial R} = -\eta\lambda_1 + (\mu + \eta)\lambda_{10},$$

$$\frac{d\lambda_{11}}{dt} = -\frac{\partial \mathcal{H}}{\partial H_t} = \mu\lambda_{11},$$

$$(26)$$

with transiversality conditions

$$\lambda_i^*\left(T_f\right) = 0, \quad i = 1, 2, \ldots, 11. \tag{27}$$

To obtain the control values, we compute the partial derivative of the Hamiltonian, given by:

$$\frac{\partial \mathcal{H}}{\partial u_i} = 0, \text{ for } i = 1, 2, 3, 4 \tag{28}$$

Moreover, the corresponding optimal controls with the boundary condition of each control $\mathfrak{u}_1^*(t),\ \mathfrak{u}_2^*(t),\ \mathfrak{u}_3^*(t),\ \text{and}\ \mathfrak{u}_4^*(t)$ are given by

$$\mathfrak{u}_1^*(t) = \max\left\{0,\ min\left\{\frac{\lambda_H^* S^*(\lambda_6 - \lambda_1) + \lambda_H^* C_q^*(\lambda_6 - \lambda_2) + \lambda_H^* C_v^*(\lambda_6 - \lambda_4) + \upsilon\lambda_H^* C_i^*(\lambda_8 - \lambda_5)}{\mathfrak{B}_1}, 1\right\}\right\},$$

$$\mathfrak{u}_2^*(t) = \max\left\{0,\ min\left\{\frac{\lambda_C^* S^*(\lambda_5 - \lambda_1) + \lambda_C^* H_p^*(\lambda_5 - \lambda_3) + \varepsilon\lambda_C^* C_v^*(\lambda_5 - \lambda_4) + \phi_1\lambda_C^* H_u^*(\lambda_8 - \lambda_6) + \phi_2\lambda_C^* H_p^*(\lambda_9 - \lambda_7)}{\mathfrak{B}_2}, 1\right\}\right\}$$

$$\mathfrak{u}_3^*(t) = \max\left\{0,\ min\left\{\frac{\Theta_1 M_u^*(\lambda_8 - \lambda_6) + \Theta_2 M_a^*(\lambda_9 - \lambda_7) + \kappa C_i^*(\lambda_5 - \lambda_{10})}{\mathfrak{B}_3}, 1\right\}\right\},$$

$$\mathfrak{u}_4^*(t) = \max\left\{0,\ min\left\{\frac{\gamma H_p^*(\lambda_7 - \lambda_{11})}{\mathfrak{B}_4}, 1\right\}\right\}.$$

(29)

From the previous analysis, to get the optimal point, we have to solve the system

$$\dot{S}^* = k_1\Delta + \alpha_1 C_q^* + \alpha_2 H_p^* + \rho C_v^* + \eta R^* - (1 - \mathfrak{u}_1^*)\lambda_H^* S^* - (1 - \mathfrak{u}_2^*)\lambda_C^* S^* - \mu S^*,$$

$$\dot{C}_q^* = k_2\Delta - ((1 - \mathfrak{u}_1^*)\lambda_H^* + \alpha_1 + \mu)C_q^*,$$

$$\dot{H}_p^* = k_3\Delta - (\alpha_2 + \mu + (1 - \mathfrak{u}_2^*)\lambda_C^*)H_p^*,$$

$$\dot{C}_v^* = k_4\Delta - (\rho + \mu + (1 - \mathfrak{u}_1^*)\lambda_H^* + \varepsilon(1 - \mathfrak{u}_2^*)\lambda_C^*)C_v^*,$$

$$\dot{C}_i^* = (1 - \mathfrak{u}_2^*)\lambda_C^* S^* \lambda_C^* H_p^* + \varepsilon(1 - \mathfrak{u}_2^*)\lambda_C^* H_p^* - \upsilon(1 - \mathfrak{u}_1^*)\lambda_H^* C_i^* - (\mu + d_1 + \mathfrak{u}_3^*\kappa)C_i^*,$$

$$\dot{H}_u^* = (1 - \mathfrak{u}_1^*)\lambda_H^* S^* + (1 - \mathfrak{u}_1^*)\lambda_H^* C_q^* + (1 - \mathfrak{u}_1^*)\lambda_H^* C_v^* + \mathfrak{u}_3^*\theta_1 M_u^* - (1 - \mathfrak{u}_2^*)\phi_1\lambda_C^* H_u^* - (\theta + \mu + d_2)H_u^*,$$

$$\dot{H}_a^* = \Theta H_u^* + \mathfrak{u}_3^*\Theta_2 M_a^* - (1 - \mathfrak{u}_2^*)\phi_2\lambda_C^* H_a^* - (\mathfrak{u}_4^*\gamma + d_3 + \mu)H_a^*,$$

$$\dot{M}_u^* = (1 - \mathfrak{u}_2^*)\phi_1\lambda_C^* H_u^* + (1 - \mathfrak{u}_1^*)\upsilon\lambda_H^* C_i^* - (\mu + d_4 + \delta + \mathfrak{u}_3^*\Theta_1)M_u^*,$$

$$\dot{M}_a^* = \delta M_u^* + (1 - \mathfrak{u}_2^*)\phi_2\lambda_C^* H_a^* - (\mu + d_5 + \mathfrak{u}_3^*\theta_2)M_a^*,$$

$$\dot{R}^* = \mathfrak{u}_3^*\kappa C_i^* - (\mu + \eta)R^*,$$

$$\dot{H}_t^* = \mathfrak{u}_4^*\gamma A_7^* - \mu H_t^*,$$

with the Hamiltonian

$$\mathcal{H} = \mathfrak{w}_1 C_i^* + \mathfrak{w}_2 H_a^* + \mathfrak{w}_3 M_u^* + \mathfrak{w}_4 M_a^* + \frac{\mathfrak{B}_1}{2}(\mathfrak{u}_1^*)^2 + \frac{\mathfrak{B}_2}{2}(\mathfrak{u}_2^*)^2 + \frac{\mathfrak{B}_3}{2}(\mathfrak{u}_3^*)^2 + \frac{\mathfrak{B}_4}{2}(\mathfrak{u}_4^*)^2 + \lambda_1(k_1\Delta + \alpha_1 C_q^* + \alpha_2 H_p^* + \rho C_v^* + \eta R^* -$$

$$(1 - \mathfrak{u}_1^*)\lambda_H^* S^* - (1 - \mathfrak{u}_2^*)\lambda_C^* S^* - \mu S^*)$$

$$+\lambda_2\left(k_2\Delta - ((1 - \mathfrak{u}_1^*)\lambda_H^* + \alpha_1 + \mu)C_q^*\right) + \lambda_3(k_3\Delta - (\alpha_2 + \mu + (1 - \mathfrak{u}_2^*)\lambda_C^*)H_p^*) + \lambda_4(k_4\Delta - (\rho + \mu + (1 - \mathfrak{u}_1^*)\lambda_H^* + \varepsilon(1 - \mathfrak{u}_2^*)\lambda_C^*)C_v^*) +$$

$$\lambda_5((1 - \mathfrak{u}_2^*)\lambda_C^* S^* + (1 - \mathfrak{u}_2^*)\lambda_C^* H_p^* + \varepsilon(1 - \mathfrak{u}_2^*)\lambda_C^* H_p^* - \upsilon(1 - \mathfrak{u}_1^*)\lambda_H^* C_i^* - (\mu + d_1 + \mathfrak{u}_3^*\kappa)C_i^*) +$$

$$\lambda_6\left((1 - \mathfrak{u}_1^*)\lambda_H^* S^* + (1 - \mathfrak{u}_1^*)\lambda_H^* C_q^* + (1 - \mathfrak{u}_1^*)\lambda_H^* C_v^* + \mathfrak{u}_3^*\theta_1 M_u^* - (1 - \mathfrak{u}_2^*)\phi_1\lambda_C^* H_u^* - (\theta + \mu + d_2)H_u^*\right)$$

$$+\lambda_7(\theta H_u^* + \mathfrak{u}_3^*\theta_2 M_a^* - (1 - \mathfrak{u}_2^*)\phi_2\lambda_C^* H_a^* - (\mathfrak{u}_4^*\gamma + d_3 + \mu)H_a^*) + \lambda_8((1 - \mathfrak{u}_2^*)\phi_1\lambda_C^* H_u^* + (1 - \mathfrak{u}_1^*)\upsilon\lambda_H^* H_u^* - (\mu + d_4 + \delta + \mathfrak{u}_3^*\theta_1)M_u^*)$$

$$+\lambda_9(\delta M_u^* + (1 - \mathfrak{u}_2^*)\phi_2\lambda_C^* H_a^* - (\mu + d_5 + \mathfrak{u}_3^*\theta_2)M_a^*) + \lambda_{10}(\mathfrak{u}_3^*\kappa H_u^* - (\mu + \eta)R^*) + \lambda_{11}(\mathfrak{u}_4^*\gamma H_a^* - \mu H_t^*),$$

where

$$\lambda_H^* = \frac{\beta_1}{N}\left(H_u^*(t) + \rho_1 H_a^*(t) + \rho_2 M_u^*(t) + \rho_3 M_a^*(t)\right) \text{ and } \lambda_C^* = \beta_2\left(H_u^*(t) + \omega_1 M_u^*(t) + \omega_2 M_a^*(t)\right).$$

5. Numerical results

In this section we have presented the numerical result we have obtained using the parameters value collected in Table 3 below. We have collected data from a variety of sources, and have compiled the values in the table for the convenience of the constructed model numerical simulations and to verify the analytical results.

5.1. Numerical simulations and discussions of the deterministic model (3)

In this section, a numerical simulation of the entire HIV/AIDS and COVID-19 co-infection model given in Eq (3) is performed. We used ode45 fourth order Runge-Kutta scheme to examine the effect of various parameters on the spread and control of COVID-19 mono-infection, HIV/AIDS mono-infection, and HIV/AIDS and COVID-19 co-infection. The parameter

Table 3. Parameter values used for the co-infection model simulation.

Symbol	Value	Source
Δ	2500	[32]
μ	0.019	[32]
α_1	0.31	Assumed
α_2	0.43	Estimated from [1]
d_1	0.33	[39]
d_2	0.315	[26]
θ	0.21	[43]
θ_1	0.30	[43]
θ_2	0.30	[43]
θ_3	0.38	Assumed
v	0.3	[43]
ϕ_1	1	[43]
ϕ_2	1	[43]
ρ_1	1.25	Assumed
ρ_2	1.5	Assumed
ρ_2	1.8	Assumed
γ	0.2	[10]
d_3	0.34	Assumed
d_4	0.42	Assumed
d_5	0.51	Assumed
η	0.200	[26]
δ	0.53	Assumed
ε	0.002	[14]
β_1	0.3425	[43]
β_2	0.1175	[43]
ω_1	1.1	Assumed
ω_2	1.4	Assumed
k_1	0.40	[27]
k_2	0.20	Assumed
k_3	0.20	Assumed
k_4	0.20	Assumed
ρ	0.30	Assumed
κ	0.05	[23]
υ	0.85	Assumed

https://doi.org/10.1371/journal.pone.0284759.t003
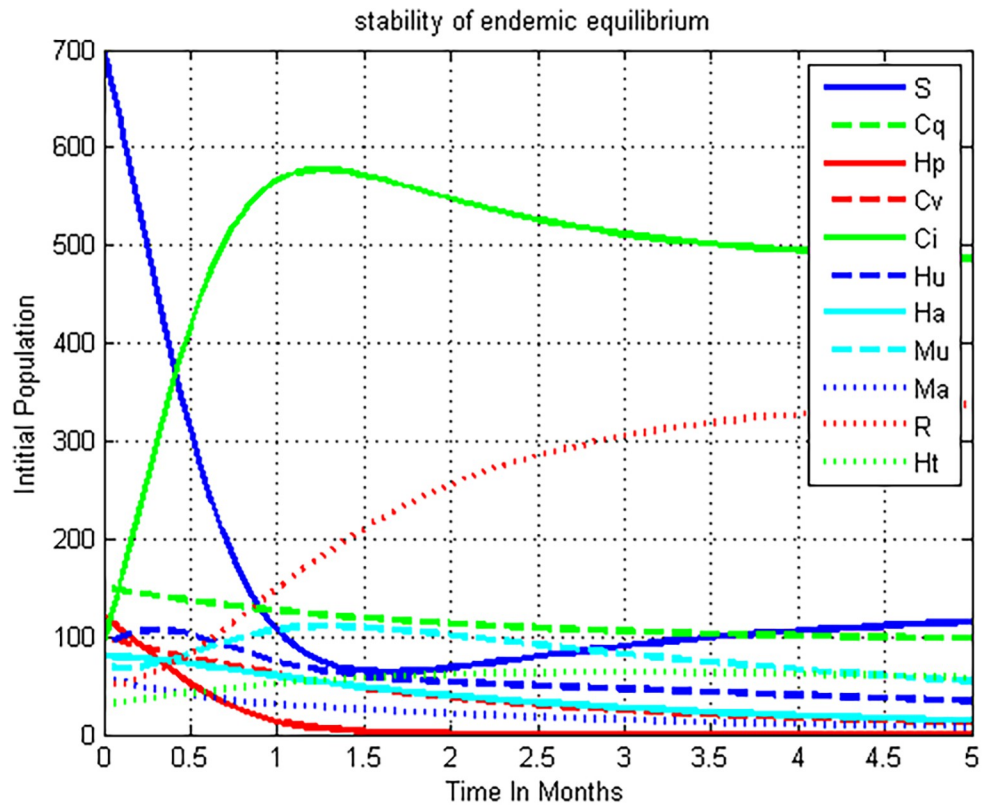
Fig 3. The feature of the co-infection model (3) solutions at $\mathcal{R}_0^{HC} = 3.2 > 1$.

values presented in Table 3 are used for numerical simulation. Moreover, we have investigated the stability of the endemic equilibrium point of the co-infection model (3), the effects of parameter on reproduction numbers, and the impact of treatment primarily on dually-infected individuals in the community.

5.2. Simulation of co-infection model (3) whenever $\mathcal{R}_0^{HC} = 3.2 > 1$

The above Fig 3 was plotted using ode45 Runge-Kutta fourth order method to observe the numerical simulation of the full co-infection model (3) by using parameter values from Table 3. We can deduce from the figure that after a year, the solutions of the COVID-19 and HIV/AIDS co-infection dynamical system (3) are approaching the endemic equilibrium point of the given dynamical system whenever the co-infection effective reproduction number $\mathcal{R}_0^{HC} = \max\{\mathcal{R}_{HM}, \mathcal{R}_{CM}\} = \max\{2, 3.2\} = 3.2 > 1$.

5.3. Numerical simulation to show the effect of k_3 on $\mathcal{R}_{HM}$

The effect of the HIV protection rate on the HIV/AIDS effective reproduction number $\mathcal{R}_{HM}$ is depicted in Fig 4. The graph shows that as the value of protection rate k_3 increases, the effective reproduction number $\mathcal{R}_{HM}$ decreases and for $k_3 > 0.771$ indicates that $\mathcal{R}_{HM}$ is reduced to less than one. As a result, the public health and policymakers must focus on increasing the values of the HIV/AIDS protection rate k_3 in order to control HIV/AIDS spread which may causes for existence of co-infection in the community.
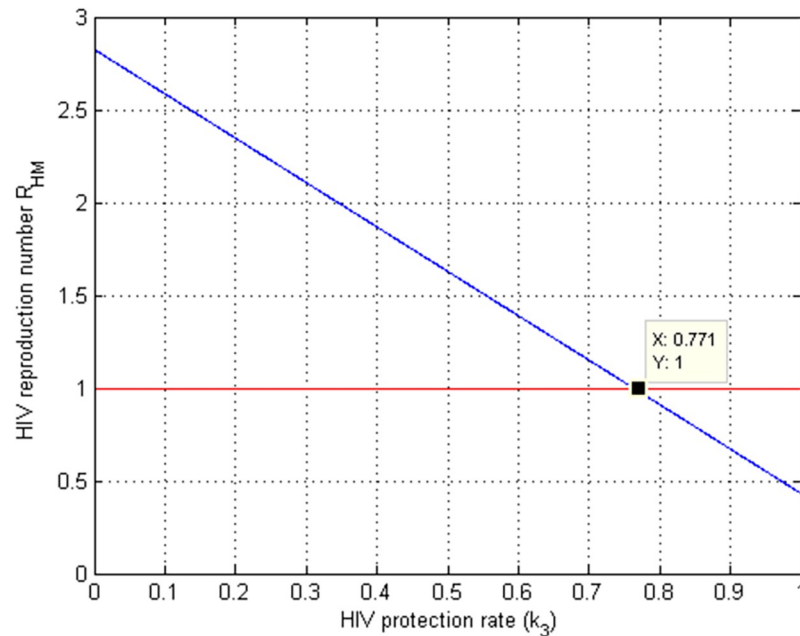
Fig 4. Simulation of HIV protection rate k3 versus $\mathcal{R}_{HM}$.

5.4. Simulation to show the effect of κ on $\mathcal{R}_C$

A numerical simulation in order to show the effect of COVID-19 treatment on the COVID-19 effective reproduction number $\mathcal{R}_C$ is given by Fig 5. The graph shows that as the value of the treatment rate raises, the COVID-19 basic reproduction number decreases and for the value of $\kappa > 0.776$ implies that $\mathcal{R}_C < 1$.
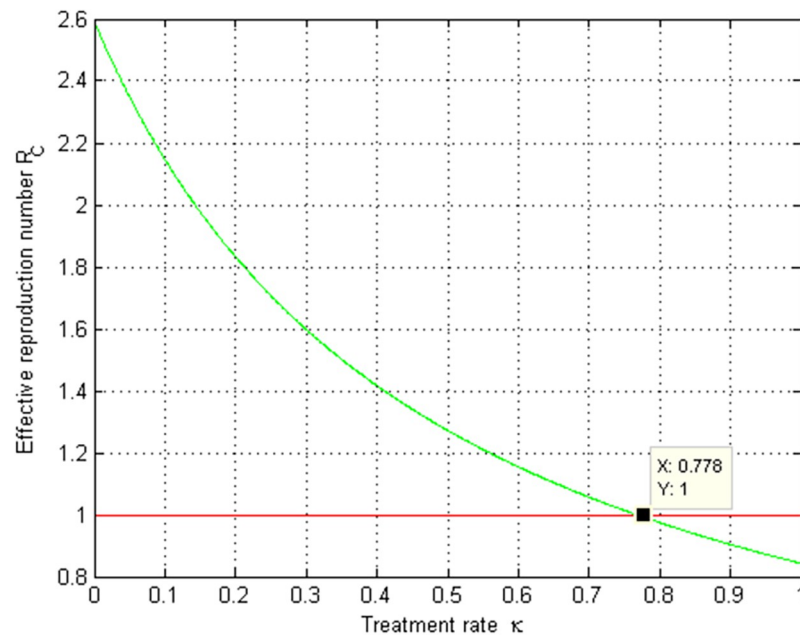
Fig 5. Simulation of COVID-19 treatment rate κ versus $\mathcal{R}_C$.
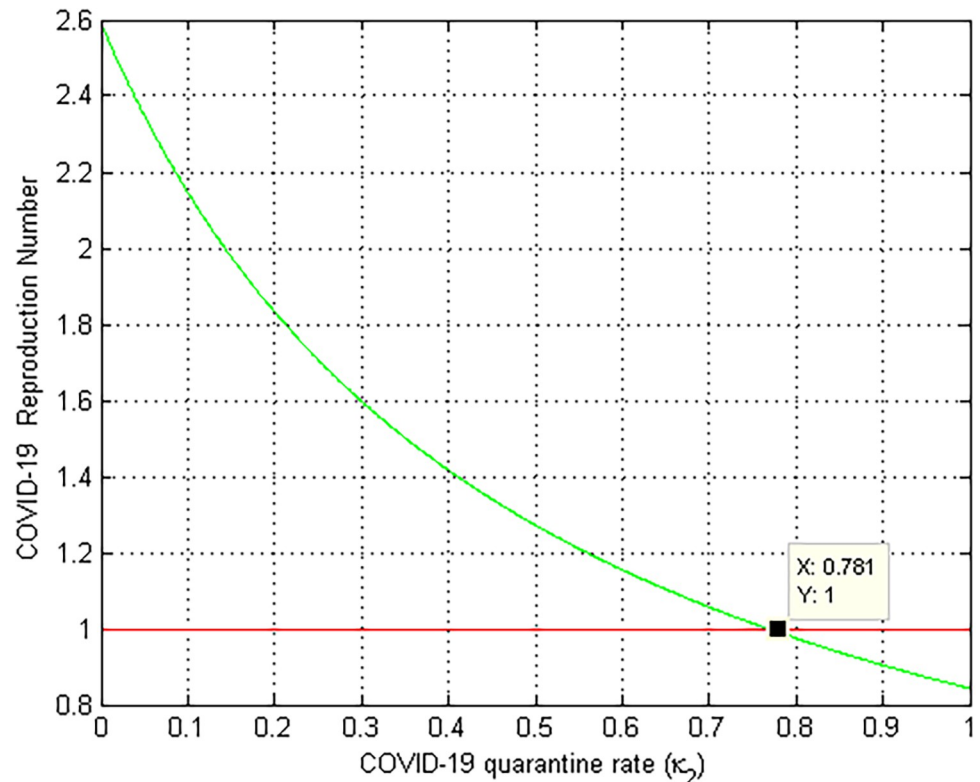
Fig 6. Numerical simulation of COVID-19 protection rate k_2 versus $\mathcal{R}_{CM}$.

5.5. Numerical simulation to show the effect of k_2 on $\mathcal{R}_{CM}$

Fig 6 depicted the effect of the COVID-19 protection rate k_2 on the COVID-19 effective reproduction number $\mathcal{R}_C$. As we can observe from the graph as the value of k_2 increases, the COVID-19 effective reproduction number decreases, and $k_2 > 0.654$ implies that $\mathcal{R}_C < 1$. As a result, all the stakeholders must focus on increasing the values of COVID-19 quarantine rate k_2 in order to prevent and control COVID-19 spread in the community. Biologically, this means that COVID-19 infection decreases as the quarantine rate k_2 rises.

5.6. Numerical simulation to show effect of β_2 on $\mathcal{R}_C$

Fig 7 shows the influence of the COVID-19 transmission rate β_2 on the COVID-19 effective reproduction number $\mathcal{R}_C$. The graph shows that as the value of β_2 rises, so does the COVID-19 effective reproduction number and the value of $\beta_2 < 0.225$ means that $\mathcal{R}_C < 1$. As a result, public health authorities must focus on reducing the value of COVID-19 transmission rate β_2 in order to avoid and regulate COVID-19 spread in the community.

5.7. Simulation to show effect of β_1 on $\mathcal{R}_{HM}$

Fig 8 depicts a numerical simulation on the influence of HIV transmission rate β_1 on the HIV/AIDS effective reproduction number $\mathcal{R}_{HM}$. The graph shows that as the value of β_1 grows, so does the HIV/AIDS effective reproduction number and whenever $\beta_1 < 0.193$ significantly $\mathcal{R}_{HM}$ reduces to less than unity. Therefore it is recommendable to give an attention on minimizing the value of the HIV transmission rate β_1 to prevent and control HIV/AIDs expansion
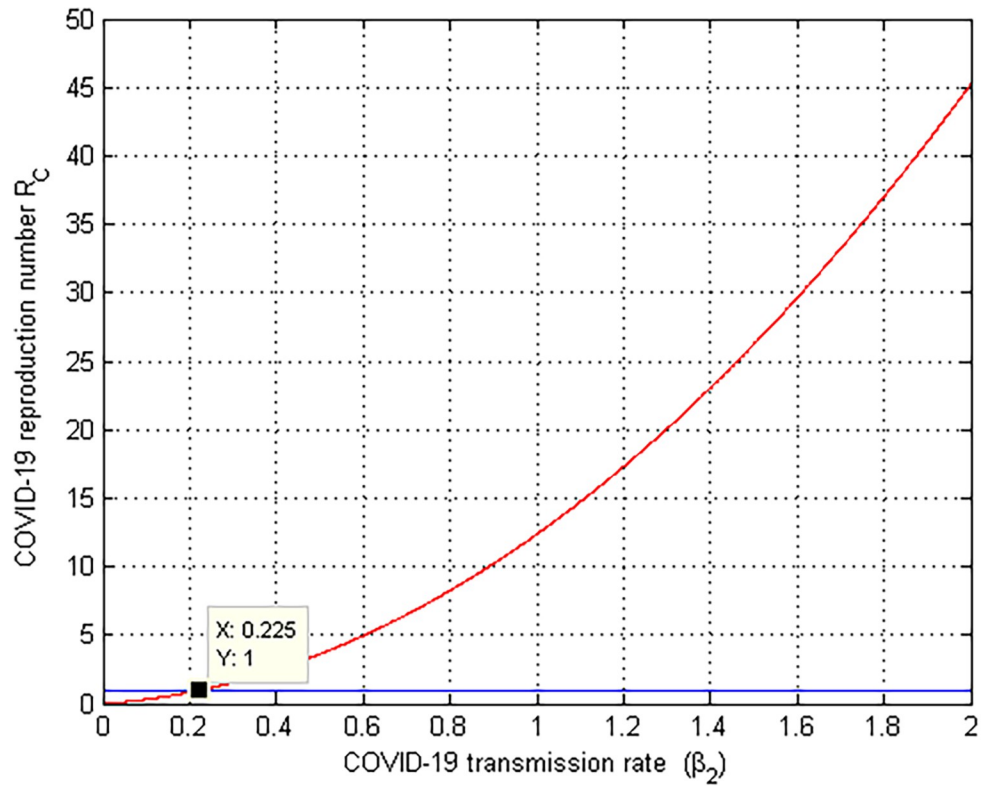
Fig 7. Numerical simulation on β_2 versus $\mathcal{R}_C$.

https://doi.org/10.1371/journal.pone.0284759.g007

Fig 8. Numerical simulation on β_1 versus $\mathcal{R}_{HM}$.

https://doi.org/10.1371/journal.pone.0284759.g008
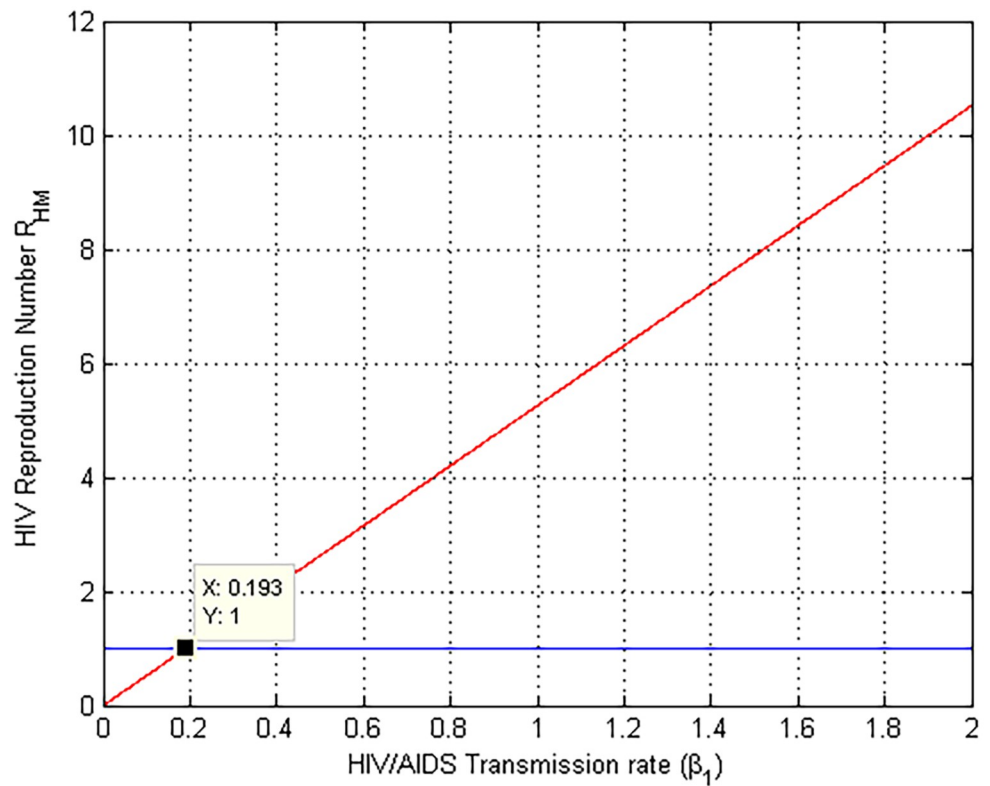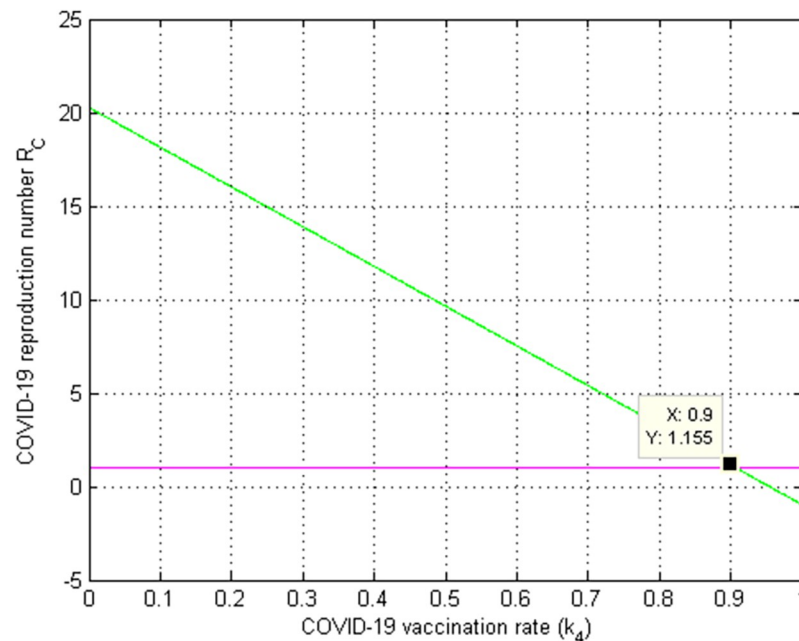
Fig 9. Numerical simulation on k_4 versus $\mathcal{R}_C$.

in the community. Biologically, this indicates that the HIV/AIDS infection lowers as the transmission rate β_1 drops.

5.8. Simulation to show effect of k_4 on $\mathcal{R}_C$

Fig 9 looked at how the COVID-19 immunization (vaccination) rate k_4 affected the COVID-19 effective reproduction number $\mathcal{R}_C$. The graph shows that when the value of k_4 grows, the COVID-19 effective reproduction number decreases, and values of $k_4 > 0.9$ suggest that $\mathcal{R}_C < 1$. As a result, public health authorities must focus on increasing the COVID-19 immunization rate k_4 in order to prevent and control COVID-19 spread in the community. Biologically, this indicates that the COVID-19 infection reduces as the immunization rate k_4 rises.

5.9. Numerical simulation to show effect of κ on COVID-19 infectious (C_i)

Fig 10 examined the effect of COVID-19 treatment rate on the number of COVID-19 mono-infectious population. The graph shows that when the value of κ increases, the number of COVID-19 mono-infectious people decrease. As a result, public officials should focus on increasing the value of the treatment rate at which COVID-19 infected individuals recovered from COVID-19 illness increase.

5.10. Simulation to show effect of θ_1 on the co-infectious (M_u)

Fig 11 looked at how θ_1 affected the number of COVID-19 and HIV/AIDS co-infected individuals. The graph shows that when the value of COVID-19 treatment rate θ_1 rises, the number of COVID-19 and HIV/AIDS co-infected individuals' decreases. As a result, public officials should focus on maximizing the value of COVID-19 treatment rate θ_1 in COVID-19 infected persons.
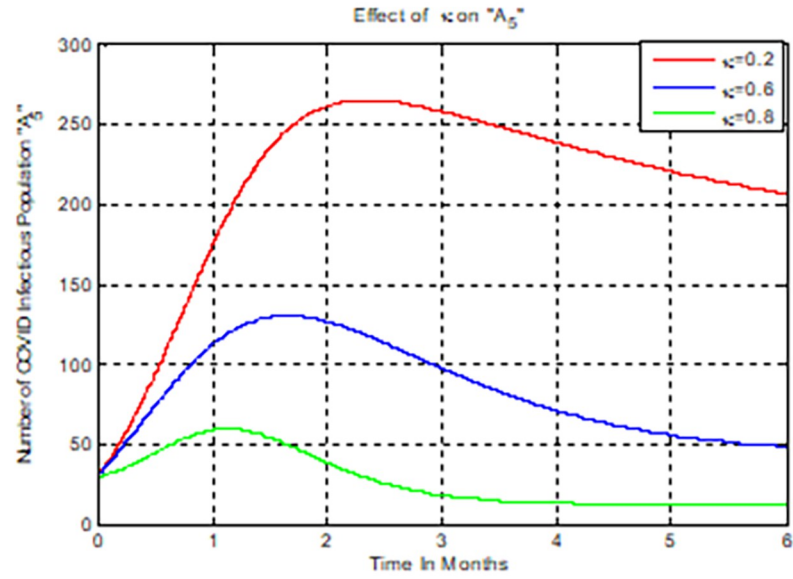
Fig 10. Numerical simulations of κ versus C_i.

Fig 11. Numerical simulation on θ_1 versus H_u.

The effect of θ₂ on Co-infected individuals those who are aware of HIV infection
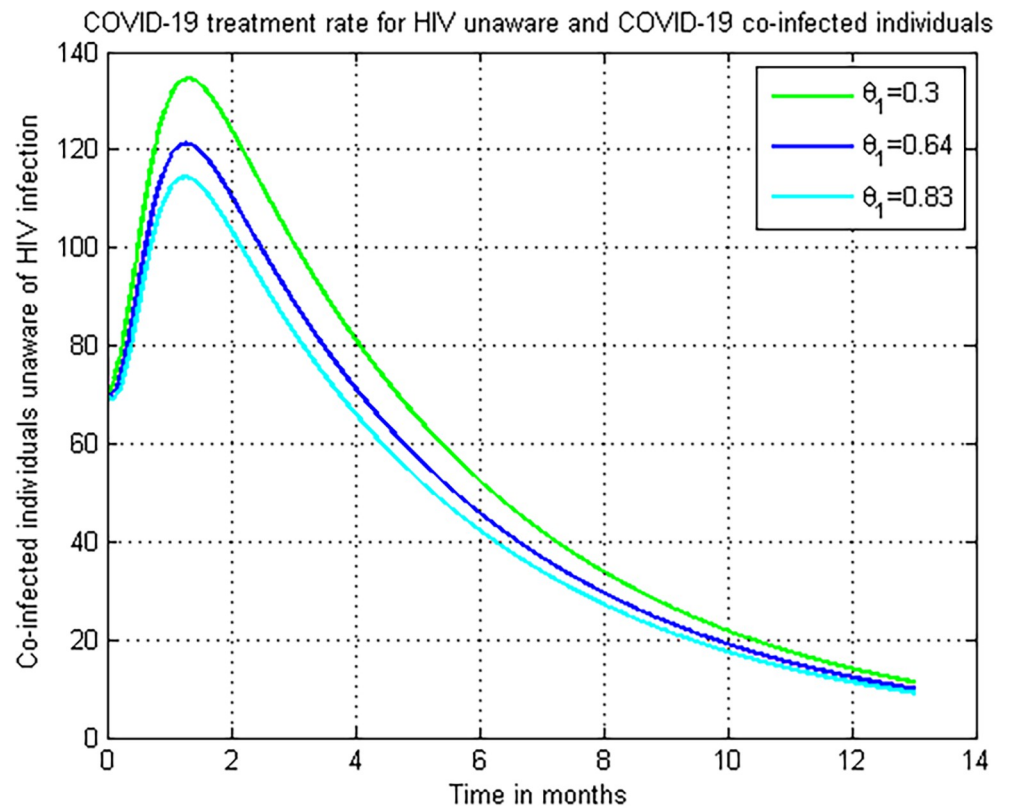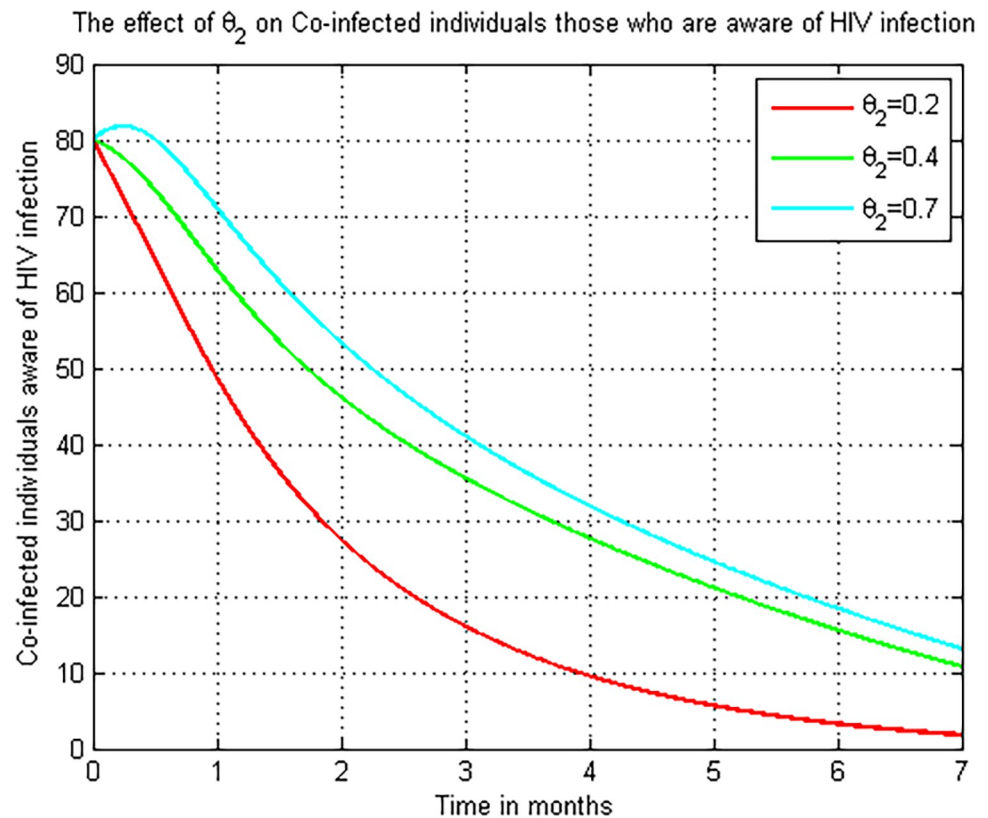
Fig 12. Numerical simulation on θ_2 versus M_a.

5.11. Simulation to show effect of θ_2 on the co-infectious (M_a)

Fig 12 show that the impact of θ_2 on the number of COVID-19 and HIV/AIDS co-infected people. The graph shows that when the value of the COVID-19 treatment rate θ_2 rises, the number of COVID-19 and HIV/AIDS co-infected individuals decrease. As a result, public officials must focus on maximizing the value of COVID-19 treatment rate θ_2 in COVID-19 infected persons.

5.12. Numerical simulations of optimal control strategies

To verify the analytical results, the optimal control model system (17) is simulated using the parameter values given in Table 3 with positive weight constants $w_1 = w_2 = w_3 = w_4 = 18$. The optimal control system is composed of two dynamical systems, the state dynamical system (17) and the adjoint dynamical system (27), each with its own initial and final-time conditions, with the control value state in Eq (26). The fourth forward-backward Runge-Kutta iterative method is used to solve this optimality system. The state Eq (17) is solved with the initial values of state variables using the fourth-order forward Runge-Kutta method. We used backward fourth order Runge-Kutta to solve the adjoint equations once we had the solution of the state functions and the value of optimal controls. To determine the impact of control measures on the reduction of the HIV/AIDS and COVID-19 co-infection we have the following three cases of optimal control strategies:

Case 1: Controlling HIV infection H_a with the combinations of strategies: strategy 1: use $u_1 = 0$, and $u_4 \neq 0$, strategy 2: use $u_1 \neq 0$, and $u_4 = 0$ and strategy 3: use $u_1 \neq 0$ and $u_4 \neq 0$.

Case 2: Controlling COVID-19 infection C_i with the combinations of strategies: strategy 1: use $u_2 = 0$, and $u_3 \neq 0$, strategy 2: use $u_2 \neq 0$, and $u_3 = 0$ and strategy 3: use $u_2 \neq 0$, and $u_3 \neq 0$.

Case 3: Controlling the total HIV/AIDS and COVID-19 co-infection $M_u + M_a$ with the combinations of strategy 1: use the strategy $u_1 = 0$, $u_2 \neq 0$, $u_3 \neq 0$, and $u_4 \neq 0$ strategy 2: use the strategy $u_1 \neq 0$, $u_2 = 0$, $u_3 \neq 0$, and $u_4 \neq 0$ strategy 3: use the strategy $u_1 \neq 0$, $u_2 \neq 0$, $u_3 \neq 0$, and $u_4 \neq 0$ strategy 4: use the strategy $u_1 \neq 0$,

5.13. HIV infection (H_a) simulation with strategy 1 ($u_1 = 0$, and $u_4 \neq 0$)

In this subsection simulation is done for the HIV/AIDS infection (H_a) when there is no control strategy in place and when there is only HIV/AIDS treatment control measure. Fig 13 shows that the HIV/AIDS treatment control measure efforts are implemented then the number of individuals infected with HIV decreases throughout time to zero.

5.14. HIV infection simulation with strategy 1 ($u_1 \neq 0$, and $u_4 = 0$)

In this subsection simulation is done for the HIV/AIDS infection (H_a) when there is no control strategy in place and when there is only HIV/AIDS protection control measure. Fig 14 shows that the HIV/AIDS protection control measure efforts are implemented then the number of individuals infected with HIV decreases throughout time to zero.
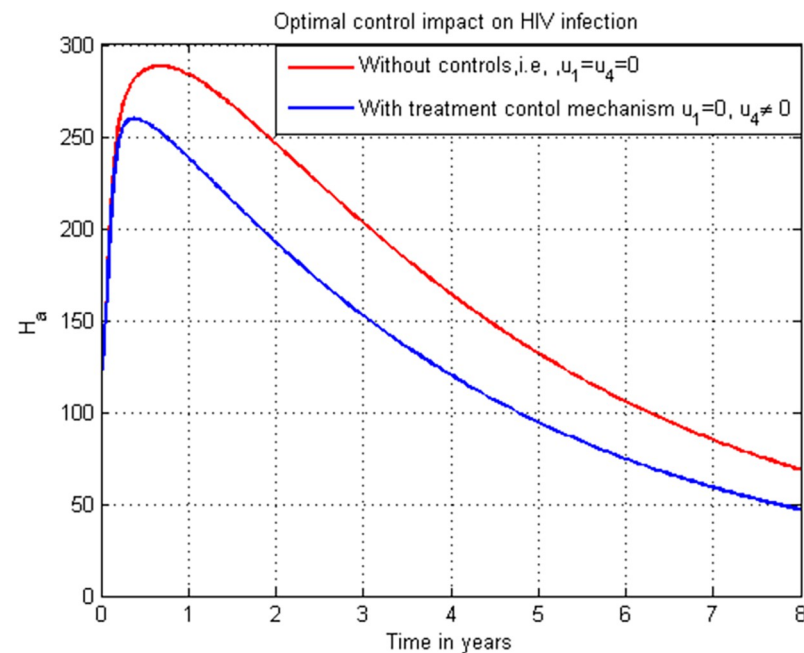
Fig 13. Simulation of HIV infection (H_a) with HIV/AIDS treatment strategy.
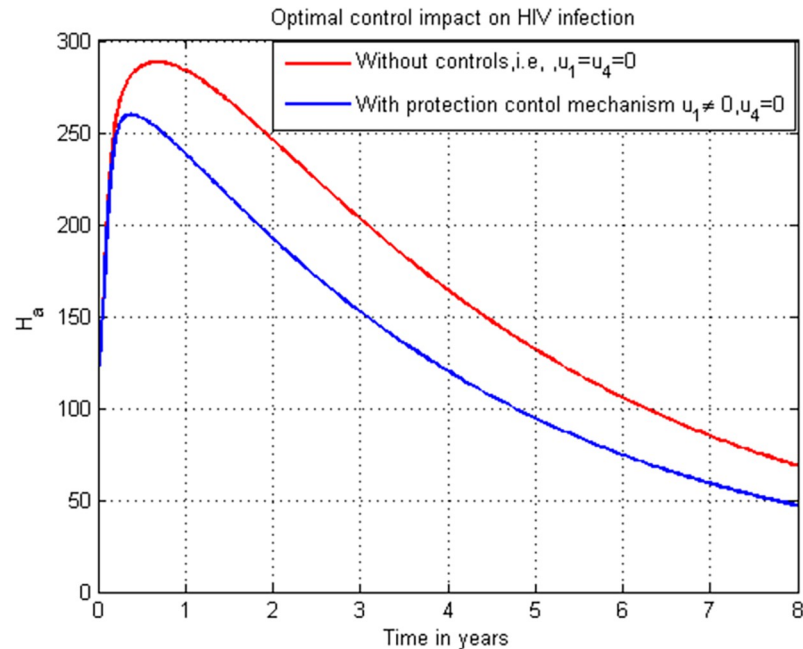
Fig 14. Simulation of HIV infection (H_a) with HIV/AIDS protection strategy.

5.15. HIV infection simulation with strategy 1 ($u_1 \neq 0$, and $u_4 \neq 0$)

In this subsection simulation is done for the HIV/AIDS infection (H_a) when there is no control strategy in place and when there are HIV/AIDS protection and treatment control measures. Fig 15 shows that the HIV/AIDS protection and treatment control measures efforts are
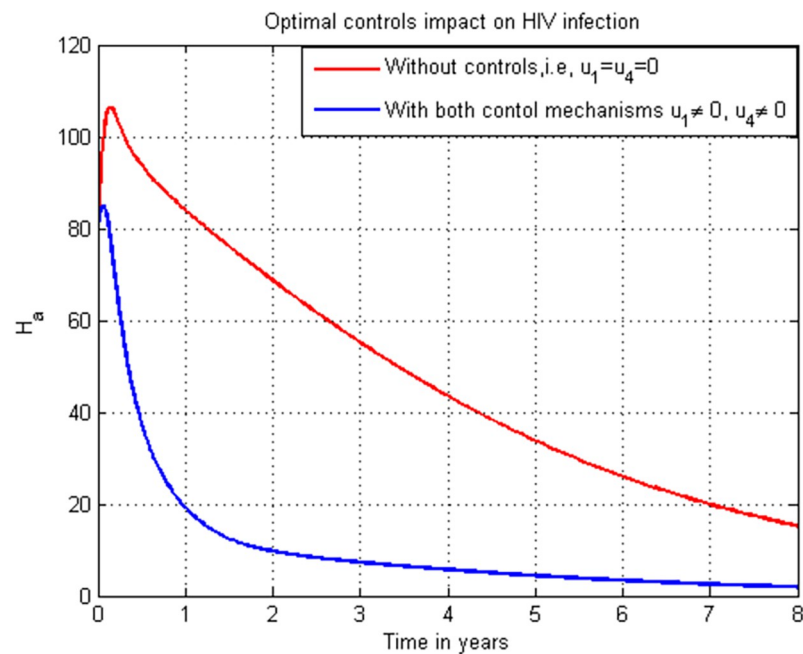

Fig 15. Simulation of HIV infection (H_a) with both HIV/AIDS protection and treatment strategies.
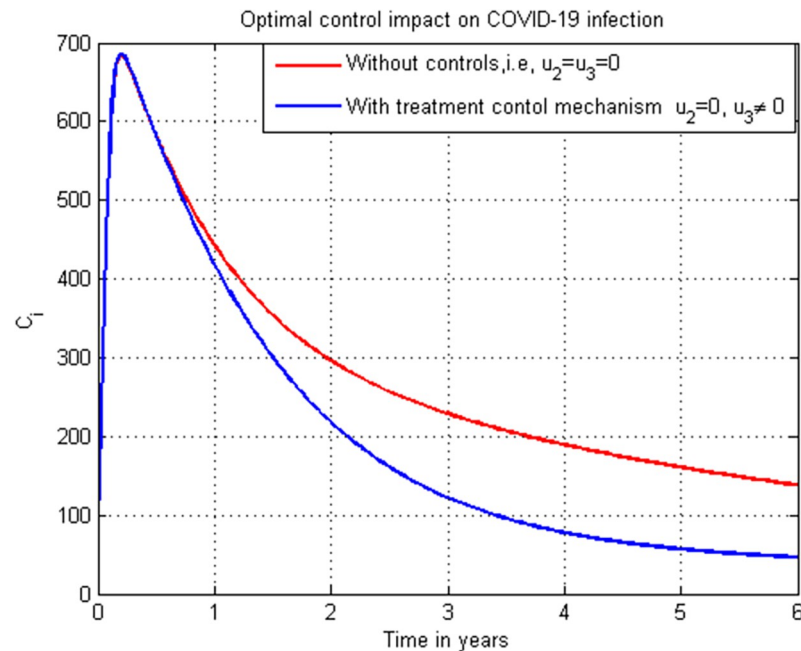
Fig 16. Simulation of COVID-19 infection (C_i) with treatment strategy.

implemented then the number of individuals infected with HIV/AIDS decreases rapidly to zero after seven years.

5.16. COVID-19 infection simulation with strategy 1 ($u_2 = 0$, and $u_3 \neq 0$)

In this subsection simulation is done for the COVID-19 infection (C_i) when there is no control strategy in place and when there is COVID-19 treatment control measure. Fig 16 shows that the COVID-19 treatment control measure effort is implemented then the number of individuals infected with COVID-19 decreases to zero through time.

5.17. COVID-19 infection simulation with strategy 1 ($u_2 \neq 0$, and $u_3 = 0$)

In this subsection simulation is done for the COVID-19 infection (C_i) when there is no control strategy in place and when there is COVID-19 protection control measure. Fig 17 shows that the COVID-19 protection control measure effort is implemented then the number of individuals infected with COVID-19 decreases to zero after five years.

5.18. COVID-19 infection simulation with strategy 1 ($u_2 \neq 0$, and $u_3 \neq 0$)

In this subsection simulation is done for the COVID-19 infection (C_i) when there is no control strategy in place and when there are COVID-19 protection and treatment control measures. Fig 18 shows that the COVID-19 protection and treatment control measures efforts are implemented then the number of individuals infected with COVID-19 decreases quickly to zero.

5.19. Co-infection simulation with strategy 1 ($u_1 = 0$, $u_2 \neq 0$, $u_3 \neq 0$, and $u_4 \neq 0$)

In this subsection simulation is done for the cumulated HIV/AIDS and COVID-19 co-infection when there is no control strategy in place and when there are controls involving COVID-
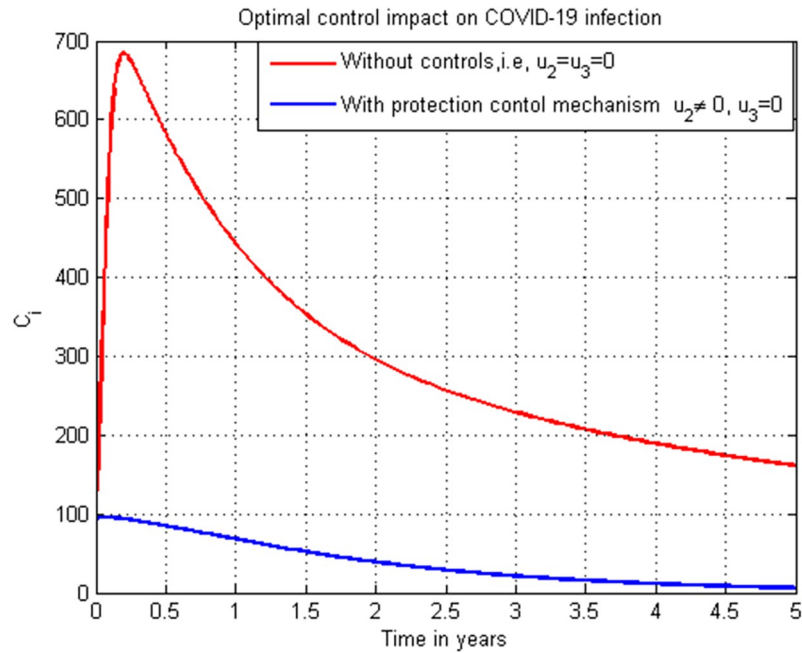
Fig 17. Simulation of COVID-19 infection (C_i) with treatment strategy.

19 protection, treatments for both HIV and COVID-19 single infections without HIV protection measure. Fig 19 shows the result that all the prevention and control strategies except HIV protection efforts are implemented, the number of individuals co-infected with HIV and COVID-19 decreases drastically to zero after year seven.
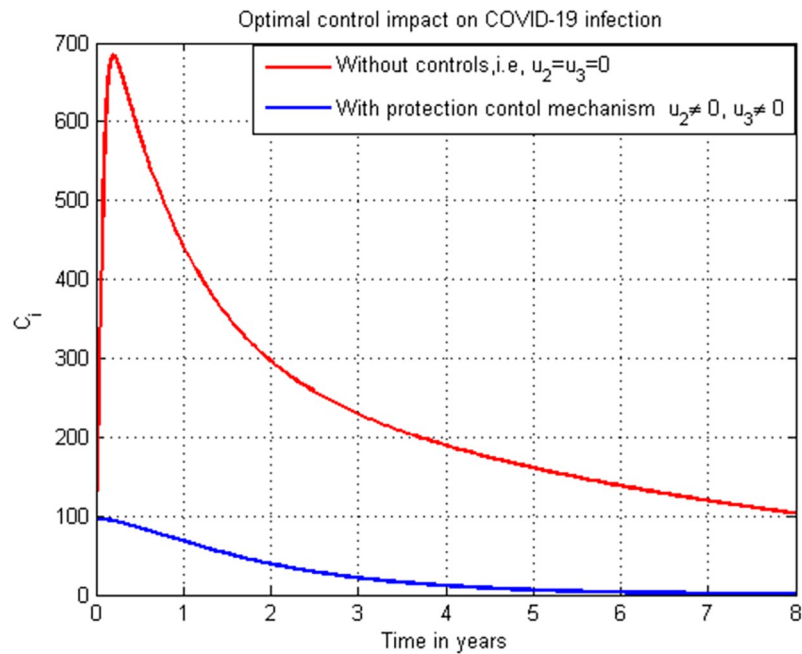

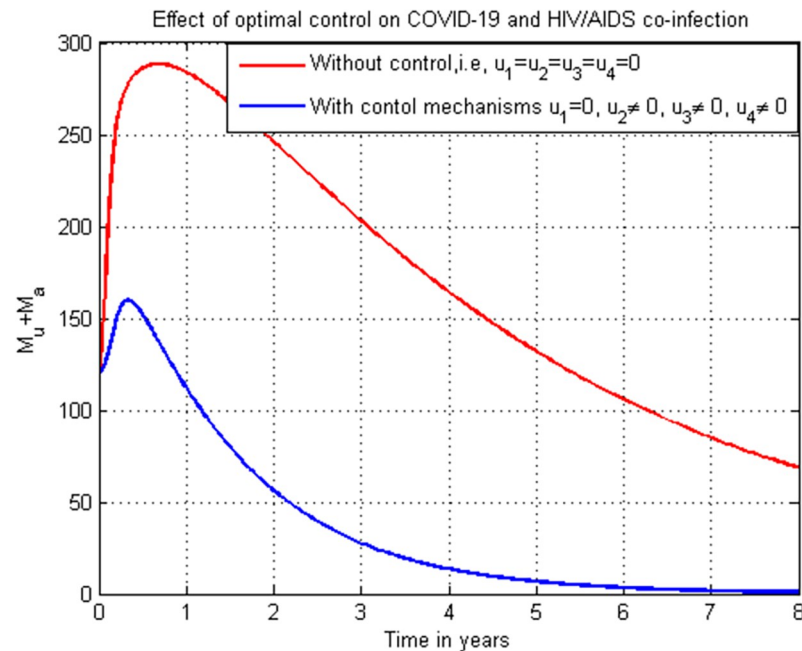**Fig 18. Simulation of COVID-19 infection (C_i) with both protection and treatment strategies.**

Fig 19. Simulation of the co-infection with COVID-19 protection and COVID-19 and HIV/AIDS treatments strategies.

5.20. Co-infection simulation with strategy 2 ($u_1 \neq 0$, $u_2 = 0$, $u_3 \neq 0$, and $u_4 \neq 0$)

In this subsection simulation is done when there is no control strategy in place and when there are controls involving HIV protection, treatment strategies for both HIV and COVID-19 single infections without COVID-19 protection measure. Fig 20 shows the result that all the prevention and control strategies except COVID-19 protection efforts are implemented, the number of individuals co-infected with HIV and COVID-19 decreases drastically to zero.

5.21. Co-infection simulation with strategy 3 ($u_1 \neq 0$, $u_2 \neq 0$, $u_3 = 0$, and $u_4 \neq 0$)

In this subsection simulation is done when there is no control strategy in place and when there are controls involving HIV protection, COVID-19 protection, and HIV treatment without COVID-19 treatment measure. Fig 21 shows the result that all the prevention and control strategies except HIV treatment strategy efforts are implemented, the number of individuals co-infected with HIV and COVID-19 decreases drastically to zero after 7 years.
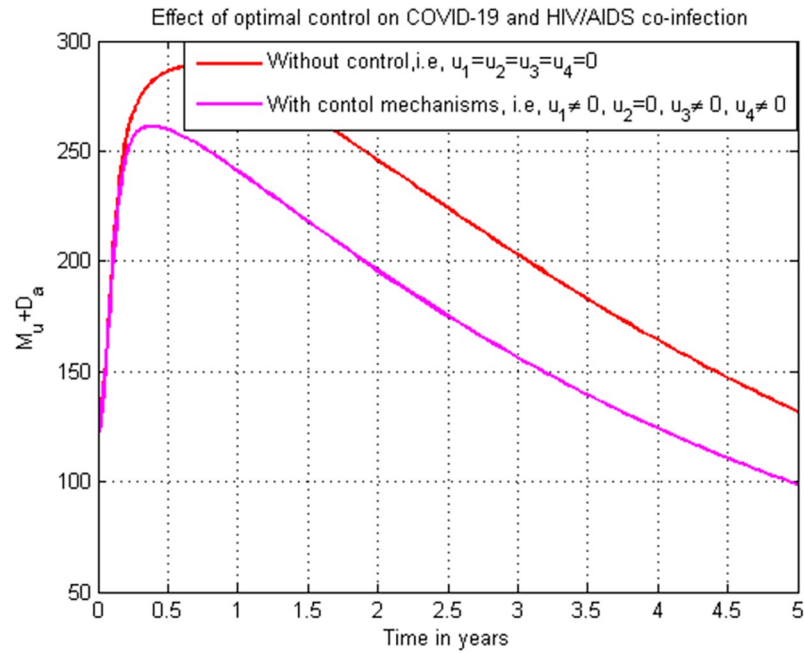
5.22. Co-infection simulation with 4 ($u_1 \neq 0$, $u_2 \neq 0$, $u_3 \neq 0$, and $u_4 = 0$)

In this subsection simulation is done when there is no control strategy in place and when there are controls involving HIV protection, COVID-19 protection, and COVID-19 treatment without HIV treatment measures. Fig 22 shows the result that all the prevention and control strategies except HIV treatment strategy efforts are implemented, the number of individuals co-infected with HIV and COVID-19 decreases drastically to zero after 8 years.

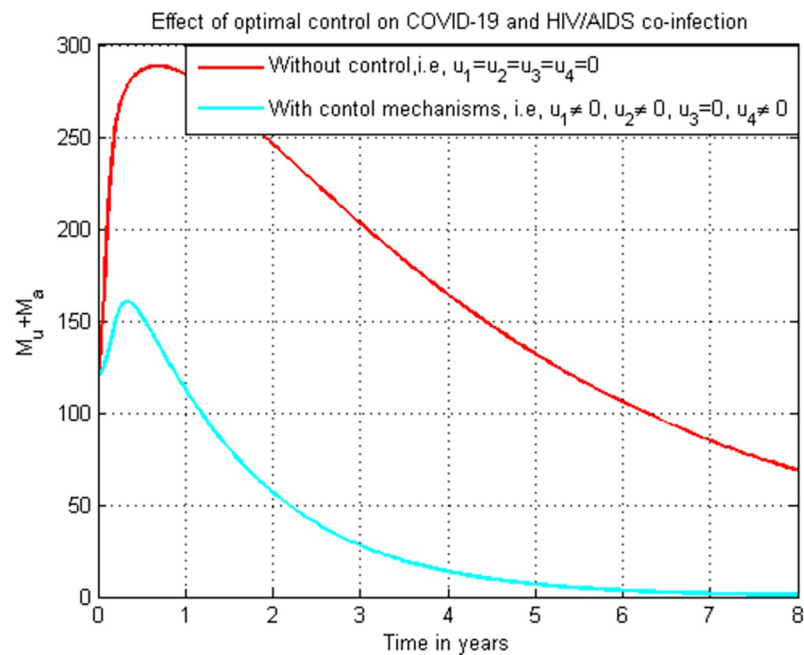**Fig 20. Simulation of the co-infection with HIV protection and COVID-19 and HIV/AIDS treatments strategies.**

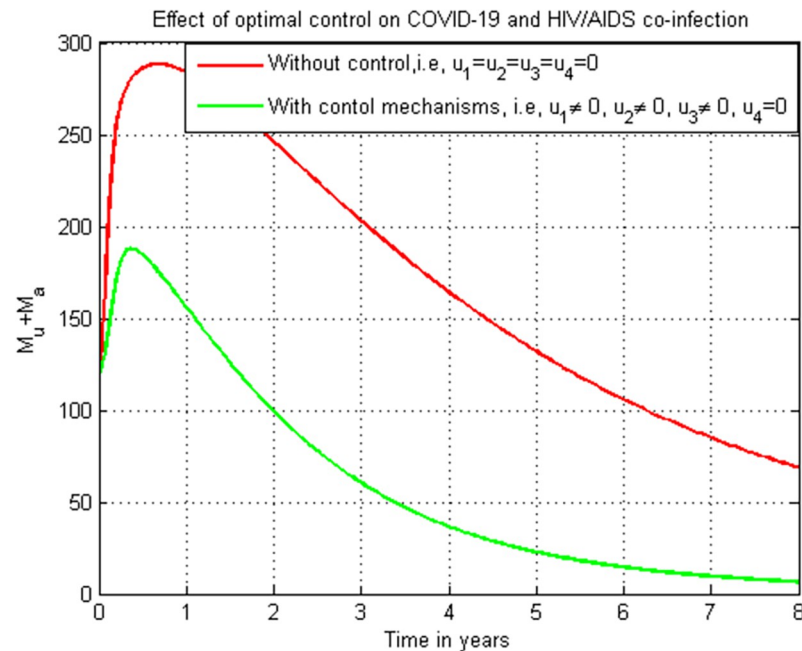**Fig 21. Simulation of the co-infection with HIV protection, COVID-19 protection and HIV/AIDS treatment strategies.**

Fig 22. Simulation of the co-infection with HIV protection, COVID-19 protection and COVID-19 treatment strategies.

5.23. Co-infection simulation with strategy 5 ($u_1 = 0$, $u_2 = 0$, $u_3 \neq 0$, and $u_4 \neq 0$)

In this subsection simulation is done when there is no control strategy in place and when there are controls involving treatment strategies for COVID-19 and HIV single infection without HIV and COVID-19 protection measures. Fig 23 shows the result that treatment strategies efforts are implemented without protection strategies, the number of individuals co-infected with HIV and COVID-19 decreases drastically to zero in the long run.

5.24. Co-infection simulation with strategy 6 ($u_1 \neq 0$, $u_2 \neq 0$, $u_3 = 0$, and $u_4 = 0$)

In this subsection simulation is done when there is no control strategy in place and when there are control strategies involving protection strategies for COVID-19 and HIV single infection without HIV and COVID-19 treatment measures. Fig 24 shows the result that protection strategies efforts are implemented without treatment strategies, the number of individuals co-infected with HIV and COVID-19 decreases drastically to zero after 8 years later.

5.25. Co-infection simulation with strategy 7 ($u_1 \neq 0$, $u_2 \neq 0$, $u_3 \neq 0$, and $u_4 \neq 0$)

In this subsection simulation is done when there is no control strategy in place and when there are all the control strategies involving protection and treatment for both COVID-19 and HIV single infections. Fig 25 shows the result that all the protection and treatment strategies efforts are implemented, the number of individuals co-infected with HIV and COVID-19 decreases drastically to zero after 3.
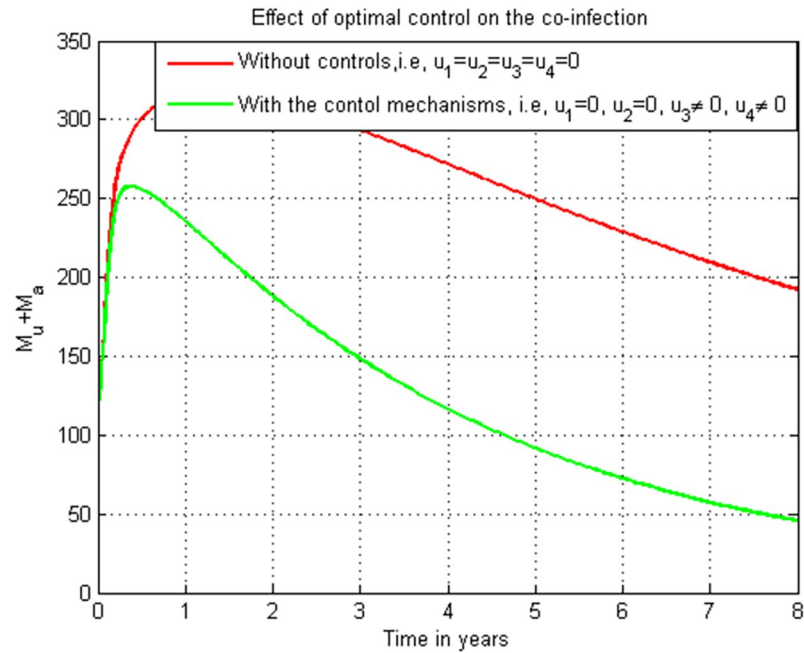
Fig 23. Simulation of the co-infection with only HIV and COVID-19 treatments strategies.

https://doi.org/10.1371/journal.pone.0284759.g023

6. Conclusions

In this paper, we formulated and investigated a continuous time dynamical model for the transmission of HIV/AIDS and COVID-19 co-infection with protection and treatment strategies. The mode incorporate four non-infectious groups the susceptible group, the HIV
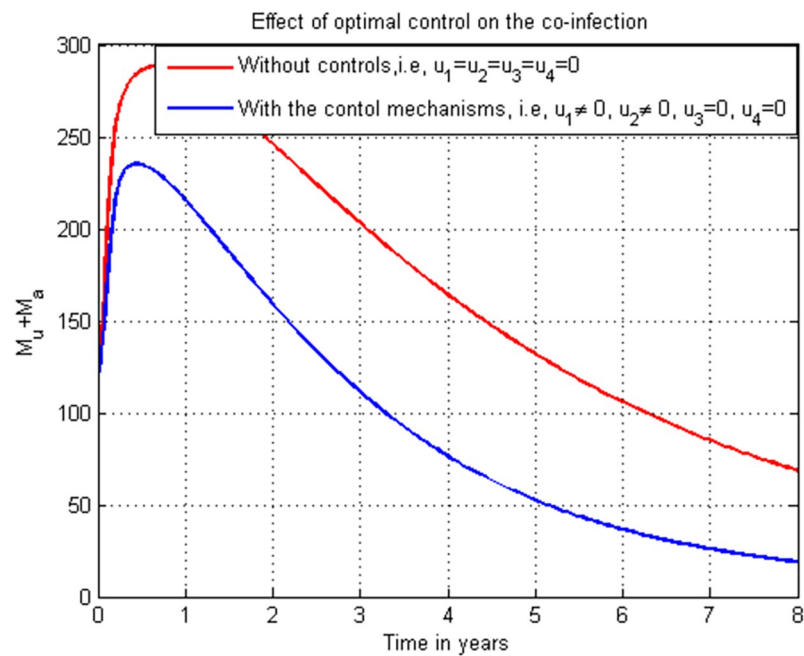

Fig 24. Simulation of the co-infection with only HIV and COVID-19 protections strategies.

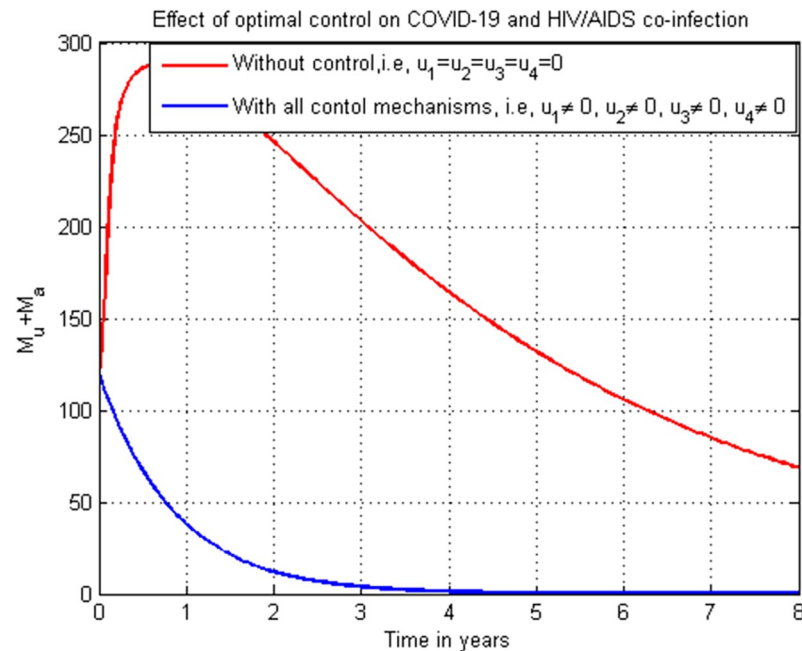https://doi.org/10.1371/journal.pone.0284759.g024

Fig 25. Simulation of the co-infection with all possible strategies.

protection group, the COVID-19 protection group, and the COVID-19 vaccinated group and this made the model highly nonlinear and challenging for the qualitative analysis of the co-infection model. The model has been mathematically analyzed both for the sub-models associating the cases that each disease type is isolated and in the case when there is co-infection. In addition an optimal control problem model that minimizes the cost of the infection as well as minimizes the control efforts to control the diseases transmission in the community is formulated and analyzed. The model includes the intervention strategies, protective as well as treatment and numerical simulations of both the deterministic model and optimal control problem models are presented. In the analysis it has been indicated that the effect of protection as well as treating the infected ones with the available treatment mechanisms affects significantly the optimal control strategy and its outcome. From the optimal control problem simulation results it can be concluded that applying both protective and treatment control mechanisms at the population level yields both economic as well as epidemiologic gains. Therefore, we recommended to the stake holders to give more attention and the overall optimal effort to implement both the protective as well as treatment control strategies to minimize the single infections as well as the co-infection diseases transmission in the community.

This study did not considered the stochastic method, fractional order method, impacts of the environment, structure of human age, the spatial structure, and real population primary epidemiological data. Based on these limitations potential researcher can consider to extend this study.

Acknowledgments

Author Contributions

Conceptualization: Shewafera Wondimagegnhu Teklu.

Data curation: Belela Samuel Kotola.

Formal analysis: Shewafera Wondimagegnhu Teklu, Yohannes Fissha Abebaw.

Investigation: Belela Samuel Kotola.

Methodology: Belela Samuel Kotola.

Software: Belela Samuel Kotola, Yohannes Fissha Abebaw.

Validation: Belela Samuel Kotola.

Visualization: Belela Samuel Kotola, Yohannes Fissha Abebaw.

Writing – original draft: Belela Samuel Kotola.

Writing – review & editing: Belela Samuel Kotola.

References

1. Ahmed Idris, Doungmo Goufo Emile F, Yusuf Abdullahi, Kumam Poom, Chaipanya Parin, et al. "An epidemic prediction from analysis of a combined HIV-COVID-19 co-infection model via ABC-fractional operator." *Alexandria Engineering Journal* 60, no. 3 (2021): 2979–2995.

2. Martcheva Maia. An introduction to mathematical epidemiology. Vol. 61. New York: Springer, 2015.

3. Teklu Shewafera Wondimagegnhu, and Terefe Birhanu Baye. "COVID-19 and syphilis Co-Dynamics Analysis using Mathematical Modelling Approach." *Frontiers in Applied Mathematics and Statistics* 8: 140.

4. Aggarwal Rajiv. "Stability analysis of a delayed HIV-TB co-infection model in resource limitation settings." *Chaos, Solitons & Fractals* 140 (2020): 110138.

5. Aslam Muhammad, Murtaza Rashid, Abdeljawad Thabet, Khan Aziz, Khan Hasib, and Gulzar Haseena. "A fractional order HIV/AIDS epidemic model with Mittag-Leffler kernel." *Advances in Difference Equations* 2021, no. 1 (2021): 1–15.

6. Awoke Temesgen Debas, and Kassa Semu Mitiku. "Optimal control strategy for TB-HIV/AIDS Co-infection model in the presence of behaviour modification." *Processes* 6, no. 5 (2018): 48.

7. Babaei Afshin, Jafari Hossein, and Liya Atena. "Mathematical models of HIV/AIDS and drug addiction in prisons." *The European Physical Journal Plus* 135, no. 5 (2020): 1–12.

8. Huo Hai-Feng, and Chen Rui. "Stability of an HIV/AIDS treatment model with different stages." *Discrete Dynamics in Nature and Society* 2015 (2015).

9. Nwankwo A., and Okuonghae D. "Mathematical analysis of the transmission dynamics of HIV syphilis co-infection in the presence of treatment for syphilis." *Bulletin of mathematical biology* 80, no. 3 (2018): 437–492. https://doi.org/10.1007/s11538-017-0384-0 PMID: 29282597

10. Teklu Shewafera Wondimagegnhu, and Mekonnen Temesgen Tibebu. "HIV/AIDS-pneumonia co-infection model with treatment at each infection stage: mathematical analysis and numerical simulation." *Journal of Applied Mathematics* 2021 (2021).

11. Nthiiri Joyce K., Lavi G. O., and Mayonge A. "Mathematical model of pneumonia and HIV/AIDS coinfection in the presence of protection." *Int J Math Anal* 9, no. 42 (2015): 2069–2085.

12. Omondi E. O., Mbogo R. W., and Luboobi L. S. "Mathematical analysis of sex-structured population model of HIV infection in Kenya." *Letters in Biomathematics* 5, no. 1 (2018): 174–194.

13. Seidu Baba, Makinde O. D., and Bornaa Christopher S. "Mathematical analysis of an industrial HIV/AIDS model that incorporates carefree attitude towards sex." *Acta Biotheoretica* (2021): 1–20. https://doi.org/10.1007/s10441-020-09407-7 PMID: 33502640

14. Teklu Shewafera Wondimagegnhu, and Rao Koya Purnachandra. "HIV/AIDS-Pneumonia Codynamics Model Analysis with Vaccination and Treatment." *Computational and Mathematical Methods in Medicine* 2022 (2022). https://doi.org/10.1155/2022/3105734 PMID: 35069778

15. Zeb Anwar, Alzahrani Ebraheem, Erturk Vedat Suat, and Zaman Gul. "Mathematical model for coronavirus disease 2019 (COVID-19) containing isolation class." BioMed research international 2020. https://doi.org/10.1155/2020/3452402 PMID: 32685469

16. Bae Seongman, Joon Seo Lim Ji Yeun Kim, Jung Jiwon, and Kim Sung-Han. "Transmission characteristics of SARS-CoV-2 that hinder effective control." *Immune network* 21, no. 1 (2021). https://doi.org/10.4110/in.2021.21.e9 PMID: 33728102

17. Baek Yae Jee, Lee Taeyong, Cho Yunsuk, Jong Hoon Hyun Moo Hyun Kim, Sohn Yujin, Kim Jung Ho et al. "A mathematical model of COVID-19 transmission in a tertiary hospital and assessment of the effects of different intervention strategies." *PloS one* 15, no. 10 (2020): e0241169. https://doi.org/10.1371/journal.pone.0241169 PMID: 33104736

18. Barbera Lauren K., Kamis Kevin F., Rowan Sarah E., Davis Amelia J., Shehata Soraya, Carlson Jesse J., Johnson Steven C., and Erlandson Kristine M. "HIV and COVID-19: review of clinical course and outcomes." *HIV Research & Clinical Practice* 22, no. 4 (2021): 102–118. https://doi.org/10.1080/25787489.2021.1975608 PMID: 34514963

19. Chen Tian-Mu, Rui Jia, Wang Qiu-Peng, Zhao Ze-Yu, Cui Jing-An, and Yin Ling. "A mathematical model for simulating the phase-based transmissibility of a novel coronavirus." *Infectious diseases of poverty* 9, no. 1 (2020): 1–8

20. Cirrincione Luigi, Plescia Fulvio, Ledda Caterina, Rapisarda Venerando, Martorana Daniela, Raluca Emilia Moldovan Kelly Theodoridou, and Cannizzaro Emanuele. "COVID-19 pandemic: Prevention and protection measures to be adopted at the workplace." *Sustainability* 12, no. 9 (2020).

21. Inayaturohmat Fatuh, Anggriani Nursanti, and Supriatna Asep Kuswandi. "A mathematical model of tuberculosis and COVID-19 coinfection with the effect of isolation and treatment." *Frontiers in Applied Mathematics and Statistics* (2022).

22. Mekonnen Temesgen Tibebu. "Mathematical model analysis and numerical simulation for codynamics of meningitis and pneumonia infection with intervention." *Scientific Reports* 12, no. 1 (2022): 1–22.

23. Mugisha Joseph YT, Ssebuliba Joseph, Nakakawa Juliet N., Kikawa Cliff R., and Ssematimba Amos. "Mathematical modeling of COVID-19 transmission dynamics in Uganda: Implications of complacency and early easing of lockdown." *PloS one* 16, no. 2 (2021): e0247456. https://doi.org/10.1371/journal.pone.0247456 PMID: 33617579

24. Musa Salihu S., Baba Isa A., Yusuf Abdullahi, Sulaiman Tukur A., Aliyu Aliyu I., Zhao Shi, and He Daihai. "Transmission dynamics of SARS-CoV-2: A modeling analysis with high-and-moderate risk populations." *Results in physics* 26 (2021): 104290. https://doi.org/10.1016/j.rinp.2021.104290 PMID: 34026471

25. Omame Andrew, Sene Ndolane, Nometa Ikenna, Nwakanma Cosmas I., Nwafor Emmanuel U., Iheonu Nneka O., and Okuonghae Daniel. "Analysis of COVID-19 and comorbidity co-infection model with optimal control." *Optimal Control Applications and Methods* 42, no. 6 (2021): 1568–1590. https://doi.org/10.1002/oca.2748 PMID: 34226774

26. Riyapan Pakwan, Shuaib Sherif Eneye, and Intarasit Arthit. "A Mathematical model of COVID-19 Pandemic: a case study of Bangkok, Thailand." *Computational and Mathematical Methods in Medicine* 2021 (2021). https://doi.org/10.1155/2021/6664483 PMID: 33815565

27. Sun Deshun, Long Xiaojun, and Liu Jingxiang. "Modeling the COVID-19 Epidemic With Multi-Population and Control Strategies in the United States." *Frontiers in Public Health* 9 (2021). https://doi.org/10.3389/fpubh.2021.751940 PMID: 35047470

28. Teklu Shewafera Wondimagegnhu. "Mathematical analysis of the transmission dynamics of COVID-19 infection in the presence of intervention strategies." *Journal of Biological Dynamics* 16, no. 1 (2022): 640–664 https://doi.org/10.1080/17513758.2022.2111469 PMID: 35972455

29. Wangari Isaac Mwangi, Sewe Stanley, Kimathi George, Wainaina Mary, Kitetu Virginia, and Kaluki Winnie. "Mathematical modelling of COVID-19 transmission in Kenya: a model with reinfection transmission mechanism " Computational and Mathematical Methods in Medicine 2021 (2021).

30. Tolossa Tadesse, Tsegaye Reta, Shiferaw Siraj, Wakuma Bizuneh, Ayala Diriba, Bekele Belay, and Shibiru Tesfaye. "Survival from a triple co-infection of COVID-19, HIV, and tuberculosis: a case report." *International Medical Case Reports Journal* 14 (2021): 611. https://doi.org/10.2147/IMCRJ.S326383 PMID: 34512043

31. Yang Hyun Mo, Lombardi Luis Pedro Junior, Morato Castro Fábio Fernandes, and Yang Ariana Campos. "Mathematical modeling of the transmission of SARS-CoV-2, Evaluating the impact of isolation in São Paulo State (Brazil) and lockdown in Spain associated with protective measures on the epidemic of CoViD-19." *Plos One* 16, no. 6 (2021): e0252271

32. Daniel D. O. "Mathematical model for the transmission of Covid-19 with nonlinear forces of infection and the need for prevention measure in Nigeria." *J. Infect. Dis. Epidem* 6 (2021): 158.

33. Danwang Celestin, Jean Jacques Noubiap Annie Robert, and Yombi Jean Cyr. "Outcomes of patients with HIV and COVID-19 co-infection: a systematic review and meta-analysis." *AIDS research and therapy* 19, no. 1 (2022): 1–12.

34. Gesesew Hailay Abrha, Mwanri Lillian, Stephens Jacqueline H., Woldemichael Kifle, and Ward Paul. "COVID/HIV co-infection: A syndemic perspective on what to ask and how to answer." *Frontiers in public health* 9 (2021): 193. https://doi.org/10.3389/fpubh.2021.623468 PMID: 33791266

35. Ssentongo Paddy, Heilbrunn Emily S., Ssentongo Anna E., Advani Shailesh, Chinchilli Vernon M., Nunez Jonathan J., and Du Ping. "Epidemiology and outcomes of COVID-19 in HIV-infected individuals: a systematic review and meta-analysis." *Scientific reports* 11, no. 1 (2021): 1–12.

36. Tamuzi Jacques L., Ayele Birhanu T., Shumba Constance S., Adetokunboh Olatunji O., Jeannine Uwimana-Nicol Zelalem T. Haile, Inugu Joseph, and Nyasulu Peter S. "Implications of COVID-19 in high burden countries for HIV/TB: A systematic review of evidence." *BMC infectious diseases* 20, no. 1 (2020): 1–18. https://doi.org/10.1186/s12879-020-05450-4 PMID: 33036570

37. Tchoumi S. Y., Diagne M. L., Rwezaura H., and Tchuenche J. M. "Malaria and COVID-19 co-dynamics: A mathematical model and optimal control." *Applied mathematical modelling* 99 (2021). https://doi.org/10.1016/j.apm.2021.06.016 PMID: 34230748

38. Ambrosioni Juan, José Luis Blanco Juliana M. Reyes-Urueña, Davies Mary-Ann, Sued Omar, Maria Angeles Marcos Esteban Martínez et al. "Overview of SARS-CoV-2 infection in adults living with HIV." *The lancet HIV* 8, no. 5 (2021): e294–e305. https://doi.org/10.1016/S2352-3018(21)00070-9 PMID: 33915101

39. Goudiaby M. S., Gning L. D., Diagne M. L., Dia Ben M., Rwezaura H., and Tchuenche J. M. "Optimal control analysis of a COVID-19 and tuberculosis co-dynamics model." *Informatics in Medicine Unlocked* 28 (2022): 100849. https://doi.org/10.1016/j.imu.2022.100849 PMID: 35071729

40. Hezam Ibrahim M., Foul Abdelaziz, and Alrasheedi Adel."A dynamic optimal control model for COVID-19 and cholera co-infection inYemen." *Advances in Difference Equations* 2021, no. 1 (2021).

41. Mekonen Kassahun Getnet, Obsu Legesse Lemecha, and Habtemichael Tatek Getachew. "Optimal control analysis for the coinfection of COVID-19 and TB." *Arab Journal of Basic and Applied Sciences* 29, no. 1 (2022): 175–192.

42. Mirzaei Hossein, McFarland Willi, Karamouzian Mohammad, and Sharifi Hamid. "COVID-19 among people living with HIV: a systematic review." *AIDS and Behavior* 25, no. 1 (2021): 85–92. https://doi.org/10.1007/s10461-020-02983-2 PMID: 32734438

43. Ringa N., Diagne M. L., Rwezaura H., Omame A., Tchoumi S. Y., and Tchuenche J. M. "HIV and COVID-19 co-infection: A mathematical model and optimal control." *Informatics in Medicine Unlocked* (2022): 100978. https://doi.org/10.1016/j.imu.2022.100978 PMID: 35663416

44. Zhang Jiu-Cong, Yu Xiao-Hui, Ding Xiao-Han, Ma Hao-Yu, Cai Xiao-Qing, Kang Sheng-Chao, and Xiang Da-Wei. "New HIV diagnoses in patients with COVID-19: two case reports and a brief literature review." *BMC infectious diseases* 20, no. 1 (2020): 1–10 https://doi.org/10.1186/s12879-020-05480-y PMID: 33076830

45. Kotola Belela Samuel, and Teklu Shewafera Wondimagegnhu. "A Mathematical Modeling Analysis of Racism and Corruption Codynamics with Numerical Simulation as Infectious Diseases." *Computational and Mathematical Methods in Medicine* 2022 (2022). https://doi.org/10.1155/2022/9977727 PMID: 35991135

46. Kotola Belela Samuel, Gebru Dawit Melese, and Alemneh Haileyesus Tessema. "Appraisal and Simulation on Codynamics of Pneumonia and Meningitis with Vaccination Intervention: From a Mathematical Model Perspective." *Computational and Mathematical Methods in Medicine* 2022 (2022). https://doi.org/10.1155/2022/9945047 PMID: 36479316

47. Teklu Shewafera Wondimagegnhu, and Terefe Birhanu Baye. "Mathematical modeling investigation of violence and racism coexistence as a contagious disease dynamics in a community." *Computational and mathematical methods in medicine* 2022 (2022). https://doi.org/10.1155/2022/7192795 PMID: 35928967

48. Takele Rediat. "Stochastic modelling for predicting COVID-19 prevalence in East Africa Countries." *Infectious Disease Modelling* 5 (2020): 598–607. https://doi.org/10.1016/j.idm.2020.08.005 PMID: 32838091

49. Aggarwal Rajiv, and Raj Yashi A. "A fractional order HIV-TB co-infection model in the presence of exogenous reinfection and recurrent TB." *Nonlinear Dynamics* 104 (2021): 4701–4725. https://doi.org/10.1007/s11071-021-06518-9 PMID: 34075277

50. Omame A., Abbas M., & Onyenegecha C. P. (2021), A fractional-order model for COVID-19 and tuberculosis co-infection using Atangana–Baleanu derivative. *Chaos*, *Solitons & Fractals*, 153, 111486. https://doi.org/10.1016/j.chaos.2021.111486 PMID: 34658543

51. Keno Temesgen Duressa, Makinde Oluwole Daniel, and Obsu Legesse Lemecha. "Optimal Control and Cost Effectiveness Analysis of SIRS Malaria Disease Model with Temperature Variability Factor." *Journal of Mathematical & Fundamental Sciences* 53, no. 1 (2021).

52. Keno Temesgen Duressa, Dano Lemessa Bedjisa, and Makinde Oluwole Daniel. "Modeling and Optimal Control Analysis for Malaria Transmission with Role of Climate Variability." *Computational and Mathematical Methods* 2022 (2022).

53. Asamoah Joshua Kiddy K., Okyere Eric, Abidemi Afeez, Moore Stephen E., Sun Gui-Quan, Jin Zhen, Acheampong Edward, and Gordon Joseph Frank. "Optimal control and comprehensive cost-effectiveness analysis for COVID-19." *Results in Physics* 33 (2022): 105177. https://doi.org/10.1016/j.rinp.2022.105177 PMID: 35070649

54. Okosun K.O., Makinde O.D. and Takaidza I., 2013. Impact of optimal control on the treatment of HIV/AIDS and screening of unaware infectives. *Applied mathematical modelling*, 37(6), pp.3802–3820.

55. Keno Temesgen Duressa, Obsu Legesse Lemecha, and Makinde Oluwole Daniel. "Modeling and optimal control analysis of malaria epidemic in the presence of temperature variability." *Asian-European Journal of Mathematics* 15, no. 01 (2022): 2250005.

56. Rabiu Musa, Willie Robert, and Parumasur Nabendra. "Optimal control strategies and sensitivity analysis of an hiv/aids-resistant model with behavior change." *Acta biotheoretica* 69 (2021): 543–589. https://doi.org/10.1007/s10441-021-09421-3 PMID: 34331152

57. Teklu Shewafera Wondimagegnhu, and Terefe Birhanu Baye. "Mathematical modeling analysis on the dynamics of university students animosity towards mathematics with optimal control theory." *Scientific Reports* 12, no. 1 (2022): 1–19

58. Abba B. Gumel, Lubuma Jean M.-S., Sharomi Oluwaseun, and Terefe Yibeltal Adane. "Mathematics of a sex-structured model for syphilis transmission dynamics." *Mathematical Methods in the Applied Sciences* 41, no. 18 (2018): 8488–8513.

59. Bakare E. A., and Nwozo C. R. "Bifurcation and sensitivity analysis of malaria–schistosomiasis co-infection model." *International Journal of Applied and Computational Mathematics* 3, no. 1 (2017).

60. Castillo-Chavez Carlos, and Song Baojun. "Dynamical models of tuberculosis and their applications." Mathematical Biosciences & Engineering 1, no. 2 (2004): 361. https://doi.org/10.3934/mbe.2004.1.361 PMID: 20369977

61. Castillo-Chavez C., Blower S., van den Driessche P., Kirschner D., & Yakubu A. A. (Eds.). (2002). *Mathematical approaches for emerging and reemerging infectious diseases*: *models*, *methods*, *and theory* (Vol. 126). Springer Science & Business Media.